

**SECTION 3****REACTOR****TABLE OF CONTENTS**

	<b>Page</b>
3.1 GENERAL SUMMARY .....	3.1-1
3.1.1 General Description .....	3.1-1
3.1.2 Principal Design Criteria .....	3.1-4
3.2 THERMAL AND HYDRAULIC CHARACTERISTICS .....	3.2-1
3.2.1 Design Basis .....	3.2-1
3.2.2 Thermal Hydraulic Design Analysis .....	3.2-2
3.3 NUCLEAR CHARACTERISTICS .....	3.3-1
3.3.1 Design Basis .....	3.3-1
3.3.2 Nuclear Design Data .....	3.3-1
3.3.3 Nuclear Design Evaluation .....	3.3-4
3.3.4 Reload Startup Physics Testing .....	3.3-5
3.4 FUEL MECHANICAL CHARACTERISTICS .....	3.4-1
3.4.1 Design Basis .....	3.4-1
3.4.2 Description of Fuel Assemblies .....	3.4-2
3.4.3 Design Evaluation .....	3.4-4
3.4.4 Surveillance and Testing .....	3.4-11
3.5 REACTIVITY CONTROL MECHANICAL CHARACTERISTICS .....	3.5-1
3.5.1 Design Basis .....	3.5-1
3.5.2 Control Methods .....	3.5-1
3.5.3 Control Rod Drive System .....	3.5-3
3.5.4 Operation and Performance Analysis .....	3.5-9
3.6 OTHER REACTOR VESSEL INTERNALS .....	3.6-1
3.6.1 Design Basis .....	3.6-1
3.6.2 Description .....	3.6-2
3.6.3 Performance Analysis .....	3.6-6

**TABLE OF CONTENTS [Continued]**

	<b>Page</b>
3.7 TESTS AND INSPECTIONS.....	3.7-1
3.7.1 Reactivity Anomalies.....	3.7-1
3.7.2 Thermal and Hydraulic Tests and Inspections .....	3.7-1
3.7.3 Core Component Tests and Inspections .....	3.7-1
3.8 REFERENCES.....	3.8-1

**LIST OF TABLES**

TABLE 3.1-1	FUEL ASSEMBLY DESIGNS
TABLE 3.2-1	THERMAL AND HYDRAULIC DESIGN PARAMETERS
TABLE 3.4-1	DELETED PER 00-318
TABLE 3.6-1	REACTOR INTERNALS ALLOWABLE STRESS CRITERIA
TABLE 3.6-2	DELETED
TABLE 3.6-3	MAXIMUM DEFLECTIONS UNDER BLOWDOWN (INCHES) (1-MILLISECOND DOUBLE-ENDED BREAK)
TABLE 3.6-4	SUMMARY OF MAXIMUM STRESS INTENSITIES (PSI) (1-MILLISECOND PIPE BREAK AND SEISMICS)

**TABLE OF CONTENTS [Continued]**

**LIST OF FIGURES**

FIGURE 3.1-1	REACTOR CORE CROSS SECTION
FIGURE 3.1-2	TYPICAL REACTOR VESSEL AND INTERNALS
FIGURE 3.1-3	TYPICAL ROD CLUSTER CONTROL ASSEMBLY
FIGURE 3.4-1	MECHANICAL STRENGTH OF ENC ZIRCALOY-4 TUBING VERSUS TEMPERATURE
FIGURE 3.4-2	MECHANICAL STRESS THRESHOLD FOR IRRADIATED ZIRCALOY CLADDING TESTED IN AN IODINE ENVIRONMENT
FIGURE 3.4-3	CYCLIC FATIGUE DESIGN CURVE FOR IRRADIATED ZIRCALOY-2 OR -4 ROOM TEMPERATURE TO 600°F (316°C). TOTAL IRRADIATION EXPOSURE $5.5 \times 10^{21}$ nvt FAST FLUENCE ( $>0.625$ eV)
FIGURE 3.5-1	CONTROL ROD DRIVE MECHANISM ASSEMBLY
FIGURE 3.5-2	CONTROL ROD DRIVE MECHANISM SCHEMATIC
FIGURE 3.6-1	LOWER CORE SUPPORT STRUCTURE
FIGURE 3.6-2	REACTOR VESSEL UPPER INTERNALS
FIGURE 3.6-3	GUIDE TUBE ASSEMBLY
FIGURE 3.6-4	DELETED
FIGURE 3.6-5	Deleted per 98134

**THIS PAGE IS LEFT INTENTIONALLY BLANK**

## **SECTION 3 REACTOR**

### **3.1 GENERAL SUMMARY**

The reactor core is made up of 121 fuel assemblies. Each fuel assembly is a canless type with the basic assembly consisting of the Rod Cluster Control (RCC) guide thimbles fastened to grids and top and bottom nozzles. The fuel rods are cold-worked stress-relief annealed ZIRLO<sup>®</sup> High Performance Fuel Cladding Material/Zircaloy or partially re-crystallized annealed Optimized ZIRLO<sup>™</sup> High Performance Fuel Cladding Material tubes containing slightly enriched uranium dioxide fuel. All fuel rods are pressurized with helium during fabrication to reduce stresses and strains and to increase fatigue life. The fuel rods are supported at several points along their length by spring-clip grids.

Full length rod cluster control assemblies are inserted into the guide thimbles of the fuel assemblies. The absorber sections of the control rods are fabricated of silver-indium-cadmium alloy encased in a cladding to prevent significant leaching of absorber material into the Reactor Coolant System (RCS). Burnable poisons are employed in the form of gadolinium oxide dispersed in a uranium dioxide matrix as part of the fuel assembly.

The control rod drive mechanisms are of the magnetic latch type. The latches are controlled by three magnetic coils. They are so designed that, upon loss of power to the coils, the rod cluster control assembly (RCCA) is released and falls by gravity to shut down the reactor.

The control rods provide sufficient control rod worth to shut the reactor down ( $k_{\text{eff}} \leq 0.99$ ) in the hot condition at any time during the life cycle with the most reactive RCCA stuck in the fully withdrawn position. Redundant equipment is provided to add soluble poison to the reactor coolant to ensure a similar shutdown capability when the reactor coolant is cooled to ambient temperatures.

The reactor is capable of meeting the performance objectives throughout core life under both steady state and transient conditions without violating the integrity of the fuel cladding. Thus the release of unacceptable amounts of fission products to the coolant is prevented.

#### **3.1.1 General Description**

The reactor core and reactor vessel internals are shown in cross-section in Figure 3.1-1 and in elevation in Figure 3.1-2. The core, consisting of the fuel assemblies and control rods, provides and controls the heat source for the reactor operation. The internals, consisting of the upper and lower core support structure, are designed to support, align, and guide the core components, direct the coolant flow to and from the core components, and to support and guide the in-core instrumentation.

01284359

The Prairie Island reactors consist of 121 fuel assemblies with a 14X14 square lattice fuel rod array. Each fuel assembly contains 179 fuel rods, 16 RCCA guide thimbles and one instrument tube. The fuel consists of cylindrical pellets of slightly enriched uranium dioxide inserted into ZIRLO/Optimized ZIRLO cladding tubes. The RCCA guide thimbles and the instrument tube are made of ZIRLO. Each assembly has seven grids of which six are located in the active fuel region. Assemblies R-90, S-70, S-98, T-69, T-73, and T-75 have the instrument tube removed.

01284359

Typically forty or more fresh assemblies are loaded each cycle. The center assembly is usually taken from the most active bundles in the spent fuel pit. All fuel rods are internally pressurized with helium during fabrication.

The control rods, designated as Rod Cluster Control Assemblies (RCCA), consist of groups of individual absorber rods which are held together by a spider at the top end and actuated as a group. In the inserted position, the absorber rods fit within hollow guide thimbles in the fuel assemblies. The guide thimbles are an integral part of the fuel assemblies and occupy locations within the regular fuel rod pattern where fuel rods have been deleted. In the withdrawn position, the absorber rods are guided and supported laterally by guide tubes which form an integral part of the upper core support structure. Figure 3.1-3 shows a typical rod cluster control assembly.

As shown in Figure 3.1-2, the fuel assemblies are positioned and supported vertically in the core between the upper and lower core plates. The core plates are provided with pins which index into closely fitting mating holes in the fuel assembly top and bottom nozzles. The pins maintain the fuel assembly alignment which permits free movement of the control rods from the fuel assembly into the guide tubes in the upper support structure without binding or restriction between the rods and their guide surfaces.

Operational or seismic loads imposed on the fuel assemblies are transmitted through the core plates to the upper and lower support structures and ultimately to the internals support ledge at the pressure vessel flange in the case of vertical loads or to the lower radial support and internals support ledge in the case of horizontal loads. The internals also provide a form fitting baffle surrounding the fuel assemblies which confines the upward flow of coolant in the core area to the fuel bearing region.

Westinghouse manufactured the fuel assemblies for Cycles 1 thru 4 for both units. The fuel assembly design was Westinghouse 14X14 STANDARD.

Exxon Nuclear Company (ENC) supplied fuel assemblies for Cycles 5 thru 10 using three different designs. The reload for Unit 1 Cycle 5 included 40 assemblies of ENC STANDARD fuel; for Unit 2 Cycle 5, the reload contained 40 fuel assemblies of ENC HIGH BURNUP design. This design increased the fuel rod cladding thickness from 0.030 inches to 0.031 inches thus increasing the fuel rod OD to 0.426 inches from 0.424. Commencing with Cycle 7, full reloads of ENC TOPROD design fuel assemblies were used. The TOPROD design had several differences from the previous designs. The changes included reduced fuel rod diameter and cladding thickness to improve neutron economy, top and bottom axial blankets to reduce neutron leakage, and gadolinia bearing fuel rods to increase core design flexibility. The mechanical and thermal hydraulic design of the ENC fuel, including those aspects affecting handling and storage, is summarized in Reference 5.

Beginning with Cycle 11 for both units, Westinghouse OFA design fuel assemblies were inserted. This design is similar to ENC TOPROD (gadolinia bearing fuel rods, axial blankets, etc.) with an exception of further reduced fuel rod diameter and clad thickness.

Beginning with Cycle 15 for both units, Westinghouse HIGH BURNUP-OFA design fuel assemblies were inserted.

Beginning with Unit 2 Cycle 16 and Unit 1 Cycle 17, Westinghouse 400 VANTAGE + design fuel assemblies were inserted. This design uses the advanced zirconium alloy material, ZIRLO, for the cladding, guide thimble and instrumentation tubes. The 400 VANTAGE + fuel design also contains gadolinia bearing fuel rods and fully enriched annular axial blankets in the non-gadolinia rods.

The ZIRLO alloy provides significant improvement in fuel rod, guide thimble tube and instrumentation tube cladding corrosion resistance and dimensional stability under irradiation (Reference 65).

Beginning with Cycle 26 for both units, Westinghouse 422 VANTAGE + design fuel assemblies were inserted. This design uses a 0.422 inch outer diameter fuel rod and instrument tube and a new mid grid designed to be compatible with the 400 VANTAGE + fuel. This fuel assembly design is described in more detail in Reference 89.

Beginning with Cycle 27 for both units, Optimized ZIRLO fuel cladding material will be used for the Westinghouse 422 VANTAGE+ fuel assemblies. Optimized ZIRLO has superior corrosion performance compared to ZIRLO (Reference 91).

Table 3.1-1 compares fuel types.

### **3.1.2 Principal Design Criteria**

#### **3.1.2.1 Reactor Core Design**

Criterion: The reactor core with its related controls and protection systems shall be designed to function throughout its design lifetime without exceeding acceptable fuel damage limits which have been stipulated and justified. The core and related auxiliary system designs shall provide this integrity under all expected conditions of normal operation with appropriate margins for uncertainties and for specified transient situations which can be anticipated. (GDC 6)

The reactor core, with its related control and protection system, is designed to function throughout its design lifetime without exceeding acceptable fuel damage limits. The core design, together with reliable process and decay heat removal systems, provides for this capability under all expected conditions of normal operation with appropriate margins for uncertainties and anticipated transient situations, including the effects of the loss of reactor coolant flow, trip of the turbine generator, loss of normal feedwater and loss of all off-site power.

The Reactor Control and Protection System is designed to actuate a reactor trip for any anticipated combination of plant conditions, when necessary, to ensure a Departure from Nucleate Boiling (DNB) does not occur.

The integrity of the fuel cladding is ensured by preventing excessive fuel swelling, excessive cladding overheating, and excessive cladding stress and strain. This is achieved by designing the fuel rods so that the following conservative limits are satisfied during normal operation or any anticipated transient condition:

- a. DNB ratio equal to or greater than the limits on which the Technical Specification Reactor Core Safety Limits are based
- b. Fuel center temperature below melting point of  $\text{UO}_2$  (Reference 68)
- c. Internal gas pressure less than that which could cause the diametral gap to increase due to outward clad creep during steady state operation or for extensive DNB propagation to occur (Reference 67)
- d. Clad stresses less than the yield stress (Reference 68)
- e. Clad strain less than 1% (Reference 68)
- f. Cumulative strain fatigue cycles less than design strain fatigue life (Reference 68)



The ability of fuel designed and operated to these criteria to withstand anticipated normal and abnormal service conditions is shown by the analyses described in Section 14 to satisfy the demands of plant operation well within applicable regulatory limits.

The reactor coolant pumps provided for the plant are supplied with sufficient rotational inertia to maintain an adequate flow coastdown in the event of a simultaneous loss of power to all pumps. The flow coastdown inertia is sufficient such that the reduction in heat flux obtained with a low flow reactor trip prevents core damage.

In the unlikely event of a turbine trip from full power without an immediate reactor trip, the subsequent reactor coolant temperature increase and volume surge to the pressurizer results in a high pressurizer pressure trip and thereby prevents fuel damage for this transient. A loss of 40.0% of nominal full load or less is normally controlled by automatic rod control together with the steam dump system to prevent a large temperature and pressure increase in the Reactor Coolant System and thus prevent a reactor trip. In this case, the overpower-temperature protection would guard against any combination of pressure, temperature and power which could result in a DNB ratio (DNBR) less than the limits on which the Technical Specification Reactor Core Safety Limits are based.

In neither the turbine trip nor the loss-of-flow events do the changes in coolant conditions provoke a nuclear power excursion because of the large system thermal inertia and relatively small void fraction. Protection circuits actuated directly by the coolant conditions identified with core limits are therefore effective in preventing core damage.

### **3.1.2.2    Suppression of Power Oscillations**

Criterion: The design of the reactor core with its related controls and protection systems shall ensure that power oscillations, the magnitude of which could cause damage in excess of acceptable fuel damage limits, are not possible or can be readily suppressed. (GDC 7)

The potential for possible spatial oscillations of core power distribution has been reviewed. In summary it is concluded that the only potential spatial instability is the xenon-induced axial instability which may be a nearly free-running oscillation with little or no inherent damping. Out-of-core instrumentation is provided to obtain necessary information concerning axial distributions. This instrumentation is adequate to enable the operator to monitor and control xenon induced oscillations. In-core instrumentation is used to periodically calibrate and verify the axial flux information provided by the out-of-core instrumentation. The analysis, detection and control of these oscillations is discussed in References 1 and 69.

**3.1.2.3 Redundancy of Reactivity Control**

Criterion: Two independent reactivity control systems, preferably of different principles, shall be provided. (GDC 27)

Two independent reactivity control systems are provided, one involving rod cluster control (RCC) assemblies described in Section 7 and the other involving the injection of a soluble poison described in Section 10.

**3.1.2.4 Reactivity Hot Shutdown Capability**

Criterion: The reactivity control systems provided shall be capable of making and holding the core subcritical from any hot standby or hot operation condition. (GDC 28)

The reactivity control systems provided are capable of making and holding the core subcritical from any hot standby or hot operating condition, including those resulting from power changes. This includes the maximum excess reactivity expected for the core, which occurs for the cold condition at the beginning of a fuel cycle.

The Rod Cluster Control (RCC) assemblies are divided into two categories comprised of control and shutdown rod groups. The control group, used in combination with soluble poison, provides reactivity control throughout the life of the core at power conditions. This group of RCC assemblies is used to compensate for short term reactivity changes, at power, from variations in reactor power requirements or coolant temperature. The soluble poison control is used to compensate for the more slowly occurring changes in reactivity throughout core life such as those due to fuel depletion and fission product buildup and for load-follow.

Upon demand for Mode 3, Hot Standby, insertion of both the control and shutdown groups of RCC assemblies will immediately make the reactor subcritical from any hot standby (Mode 2, Startup) or hot operating (Mode 1, Power Operation) condition. Subsequent injection (using Charging or Safety Injection Pumps) of soluble poison can be used to assure continuation of Mode 3, Hot Standby under all circumstances.

**3.1.2.5 Reactivity Shutdown Capability**

Criterion: One of the reactivity control systems provided shall be capable of making the core subcritical under any anticipated operating condition (including anticipated operational transients) sufficiently fast to prevent exceeding acceptable fuel damage limits. Shutdown margin should assure subcriticality with the most reactive control rod fully withdrawn. (GDC 29).

The reactor core, together with the reactor control and protection system, is designed to make the core subcritical under any anticipated operating condition (including anticipated operational transients) sufficiently fast that the minimum allowable DNBR is greater than the limits on which the Technical Specification Reactor Core Safety Limits are based and the maximum fuel temperature at design overpower does not exceed the fuel melting temperature.

The shutdown groups are provided to supplement the control group of RCC assemblies to make the reactor at least one per cent subcritical ( $k_{eff} = 0.99$ ) following a trip from any credible operating condition to the hot zero power condition assuming the most reactive RCC assembly remains in the fully withdrawn position.

Sufficient shutdown capability is also provided to maintain the core subcritical with the most reactive rod assumed to be fully withdrawn for the most severe anticipated cooldown transient associated with a spurious opening of a steam bypass or a safety valve stuck fully open (see Section 14.5.5).

#### **3.1.2.6 Reactivity Holddown Capability**

Criterion: The reactivity control systems provided shall be capable of making the core subcritical under credible accident conditions with appropriate margins for contingencies and limiting any subsequent return to power such that there will be no undue risk to the health and safety of the public. (GDC 30)

The reactivity control systems provided are capable of making and holding the core subcritical, under accident conditions, in a timely fashion with appropriate margins for contingencies. Normal reactivity shutdown capability is provided within 2 seconds following a trip signal by control rods with soluble poison (boric acid) injection used to compensate for the long term xenon decay transient and for plant cooldown. Any time that the reactor is at power, the quantity of boric acid retained in the boric acid tanks and ready for injection always exceeds that required for Mode 5, Cold Shutdown. This quantity also exceeds that required to bring the reactor to Mode 3, Hot Standby and to compensate for subsequent xenon decay.

Boric acid for each unit is pumped from a boric acid tank by boric acid transfer pumps to the suction of charging pumps which inject boric acid into the reactor coolant. Any charging pump and any boric acid transfer pump can be operated from diesel generator power on loss of outside power. Boric acid can be injected by one pump at a rate which shuts the reactor down hot with no rods inserted in less than eighty (80) minutes. In eighty (80) additional minutes, enough boric acid can be injected to compensate for xenon decay, although xenon decay below the equilibrium operating level does not begin immediately, but could occur up to 26 hours after shutdown, depending upon power history. If two boric acid pumps and two charging pumps are available, these time periods are reduced. Additional boric acid injection is employed if it is desired to bring the reactor to Mode 5, Cold Shutdown.

On the basis of the above, the injection of boric acid is shown to afford backup reactivity shutdown capability, independent of RCC Assemblies which normally serve this function in the short term situation. Shutdown for long term and reduced temperature conditions can be accomplished with boric acid injection using redundant components, thus achieving the measure of reliability implied by the criterion.

Alternately, boric acid solution at lower concentration can be supplied from the refueling water storage tank. This solution can be transferred directly by the charging pumps. The reduced boric acid concentration lengthens the time required to achieve equivalent shutdown conditions.

For added flexibility the RCS can also be supplied with boric acid solution from the safety injection (SI) pumps drawing suction from the refueling water storage tank. If necessary, the RCS can be sufficiently depressurized to allow injection using the SI Pumps.

#### **3.1.2.7 Reactivity Control Systems Malfunction**

Criterion: The reactor protection systems shall be capable of protecting against any single malfunction of the reactivity control system, such as unplanned continuous withdrawal (not ejection or dropout) of a control rod, by limiting reactivity transients to avoid exceeding acceptable fuel damage limits. (GDC 31)

The reactor protection systems are capable of protecting the reactor against any single anticipated malfunction of the reactivity control system, by limiting reactivity transients to avoid exceeding acceptable fuel damage limits.

Reactor shutdown with rods is completely independent of the normal rod control functions since the trip breakers completely interrupt the power to the latch type rod mechanisms regardless of existing control signals.

#### **3.1.2.8 Maximum Reactivity Worth of Control Rods**

Criterion: Limits, which include reasonable margin, shall be placed on the maximum reactivity worth of control rods or elements and on rates at which reactivity can be increased to ensure that the potential effects of a sudden or large change of reactivity cannot (a) rupture the reactor coolant pressure boundary or (b) disrupt the core, its support structure, or other vessel internals sufficiently to lose capability of cooling the core. (GDC 32)

The maximum reactivity worth of control rods and the maximum rates of reactivity insertion employing both control rods and boron removal are limited to values for which acceptable transient analysis results are obtained in terms of preventing rupture of the coolant pressure boundary or disruption of the core or vessel internals to a degree so as to lose capability to cool the core. Details of rod worths, reactivity insertion rates and their relationship to plant safety are included in Section 14.

The reactor control system employs control rod clusters, which are divided into shutdown and control groups. The shutdown group is fully withdrawn during power operation. The control group is used to control load and reactor coolant temperature. The rod cluster drive mechanisms are wired into preselected groups and are therefore prevented from being withdrawn in other than their respective groups. The rod drive mechanism is of the magnetic latch type and the coil actuation is sequenced to provide variable speed rod travel.

The reactivity insertion rate is analyzed in the detailed plant analysis for each cycle. It is assumed that two of the highest worth groups are accidentally withdrawn at maximum speed. (See Section 14.4.) This is to ensure that the reactivity insertion rates are well within the capability of the overpower-overtemperature protection circuits. Thus core damage is prevented.

**THIS PAGE IS LEFT INTENTIONALLY BLANK**

## **3.2 THERMAL AND HYDRAULIC CHARACTERISTICS**

### **3.2.1 Design Basis**

The reactor core is designed to meet the following limiting thermal and hydraulic criteria:

- a. The minimum allowable DNBR during normal operation and anticipated transients meets the applicable DNBR correlation limit.
- b. No fuel melting during any anticipated normal operating condition.
- c. The reload fuel must be thermally and hydraulically compatible with the existing fuel and the reactor core throughout the life cycle of the fuel.
- d. Fuel rod damage will not occur due to excessive clad oxidation and hydriding. For Unit 1, all limits on cladding oxidation can be found in Reference 96. For Unit 2, the cladding metal-oxide interface temperature shall not exceed the limits given in References 65 and 66.

01454730

To maintain fuel rod integrity and prevent fission product release, it is necessary to prevent clad overheating under all operating conditions. This is accomplished by preventing a departure from nucleate boiling (DNB) which causes a large decrease in the heat transfer coefficient between the fuel rods and the reactor coolant resulting in high clad temperatures.

The ratio of the heat flux causing DNB, as predicted by the applicable DNB correlation, to the existing heat flux at a particular core location is the DNB ratio. The heat flux causing DNB is predicted by methods and correlations in Section 14.3. A DNBR correlation limit corresponding to a 95% probability at a 95% confidence level that DNB does not occur is chosen as an appropriate limit to DNB for all operating conditions.

DNB ratio is not, however, an observable parameter during reactor operation. Therefore, the observable parameters, reactor thermal power (measured as reactor coolant system loop temperature difference across core,  $\Delta T$ ), reactor coolant temperature and pressure have been related to DNB ratio through DNB correlations. Curves presented in the Technical Specifications represent the loci of points of reactor thermal power ( $\Delta T$ ), reactor coolant pressure and reactor coolant system loop average temperature for which the DNB ratio is equal to the DNBR limit. The lines indicate the maximum permissible reactor thermal power ( $\Delta T$ ) as a function of reactor coolant pressure and reactor coolant system loop average temperature.

### **3.2.2 Thermal Hydraulic Design Analysis**

#### **3.2.2.1 Hydraulic Compatibility**

The hydraulic compatibility between 400 and 422 Westinghouse VANTAGE+ fuel assemblies have been evaluated. Characteristics of the 400 and 422 VANTAGE+ assemblies which affect hydraulics are listed in Table 3.1-1. Both assembly designs use seven grids. The grids are located at the same elevations which minimizes crossflows in the mixed cores.

Hydraulic compatibility of the 400 and 422 VANTAGE + fuel was evaluated and determined acceptable as described in Reference 89.

#### **3.2.2.2 Fuel Temperature Analysis**

The fuel temperature analysis for both 400 and 422 VANTAGE + fuel designs is given in Reference 89. The limits necessary to assure fuel melting does not occur are presented in maximum kw/ft and are confirmed on a cycle specific basis.

#### **3.2.2.3 Design Analysis Conditions and Results**

##### **Departure from Nucleate Boiling Ratio**

A departure from nucleate boiling (DNB) is characterized by an abrupt decrease in the fuel rod heat transfer due to steam blanketing at the fuel rod surface. The heat flux at which DNB occurs is termed the DNB heat flux. DNB heat flux is a function of coolant conditions, axial power distribution and fuel design parameters. In tests, the DNB heat flux is indicated by a rapid fuel rod surface temperature excursion.

In reactor design, the heat flux associated with DNB and the location of DNB are both important. The magnitude of the local fuel rod temperature after DNB depends upon the axial location where DNB occurs. The local DNB heat flux ratio, or departure from nucleate boiling ratio (DNBR), defined as the ratio of the predicted DNB heat flux to the local heat flux, is indicative of the margin available in the local heat flux before reaching DNB.

The W-3 DNB correlation (Reference 73) incorporates both local and system parameters in predicting the local DNB heat flux. This correlation includes the non-uniform axial heat flux effect and, to some extent, the upstream effect, by using the inlet enthalpy as parameter. The W-3 DNB correlation has been extensively validated against test data and shown to be conservative for the prediction of DNB in fuel rod bundle with and without mixing vane grids.



The Westinghouse WRB-1 correlation (Reference 74) is used to predict the DNB heat flux for the Westinghouse 400 and 422 VANTAGE+ fuel. The WRB-1 correlation is a linear function of the local quality with coefficients that are a function of pressure and local coolant mass flux. The correlation has a “built-in” grid factor effect (to take into account DNB enhancement due to mixing vane grids) and unheated wall factor. The correlation is also modified by a non-uniform axial heat flux factor. The WRB-1 DNB correlation and associated DNBR limit have been implemented for use with 400 and 422 VANTAGE+ fuel. The NRC has reviewed and approved the use of the WRB-1 correlation and associated DNBR limit for use with 400 and 422 VANTAGE+ fuel design (Reference 75).

Thermal-Hydraulic analyses are performed to confirm that there is 95% probability with 95% confidence level that no rod will experience DNB during Condition I and II events. For Condition III and IV events, a limited percent of rod is allowed to be in DNB as described in Section 14.4.

### **Application of the WRB-1 Correlation in Design**

In conjunction with the WRB-1 correlation, the design method employed to meet the DNB design basis is the “Revised Thermal Design Procedure” (RTDP) (Ref. 86). Uncertainties in plant operating parameters, nuclear and thermal parameters, and fuel fabrication parameters and DNBR correlation uncertainty are considered statistically in order to meet the 95/95 DNB design basis. This establishes a DNBR value which must be met in plant safety analyses. Since the parameter uncertainties are considered in determining the design DNBR value, the plant safety analyses are performed using values of input parameters without uncertainties. For 400 VANTAGE + fuel, the minimum required design DNBR values are 1.22 for thimble coldwall cells (three fuel rods and a thimble tube) and 1.22 for typical cell (four fuel rods) without consideration of rod bow and instrumentation biases. For 422 VANTAGE +fuel, the minimum required DNBR values are 1.23 for thimble coldwall cells and 1.23 for typical cell (four fuel rods) without consideration of rod bow and instrumentation biases.

### **Hot Channel Factors**

The total hot channel factors for heat flux and enthalpy rise are defined as the maximum-to-core averages ratio of these quantities. The heat flux factors consider the local maximum as a point (the “hot spot”, maximum linear power density), and the enthalpy rise factors involve the maximum integrated value along a channel (the “hot channel”).

### **Engineering Hot Channel Factors**

Each of the total hot channel factors is the product of a nuclear hot channel factor describing the neutron flux distribution and an engineering hot channel factor to allow for variations from design conditions. The engineering hot channel factors account for the effects of flow conditions and fabrication tolerances and are made up of sub-factors accounting for the influence of the variations of fuel pellet diameter, density, enrichment, and fuel rod diameter, pitch and bowing, inlet flow distribution, flow redistribution; and flow mixing.

The heat flux engineering hot channel factor,  $F_{Q}^E$ , is 1.03. Different values for each enthalpy rise engineering hot channel factor,  $F_{\Delta H}^E$ , are considered separately for each effects (see below).

#### Heat Flux Engineering Sub-factor, $F_{Q}^E$

This sub-factor, used to evaluate the maximum heat flux, is determined by statistically combining the tolerances for the fuel diameter, density, enrichment and the fuel rod diameter, pitch and bowing and has a value of 1.03. Measured manufacturing data from the first three Yankee cores, the SELNI core and Indian Point Core B showed this factor to be conservative in comparison to the value obtained for the probability limit of three standard deviations. Thus, as expected a statistical sampling of the fuel assemblies of this plant also showed this sub-factor to be conservative.

#### Enthalpy Rise Engineering Sub-Factor, $F_{\Delta H}^E$

The items considered to contribute to the enthalpy rise engineering hot channel factors are discussed below:

1. Rod-to-rod variations in enrichment and density,  $F_{\Delta H,1}^E$

The current design value of  $F_{\Delta H,1}^E$  equal 1.021 is used for Standard DNB method (based on measurements obtained from a number of fuel regions) is considered valid for all current plants. For improved DNB methods (RTDP),  $F_{\Delta H,1}^E$  is combined statistically with other uncertainties to define the DNBR limit.

2. Fuel rod outer diameter, rod pitch and bowing

Since the total nuclear peaking augmentation factor ( $F_{Q}^U$ ) described in 3.2.2.4.2 is not an input to DNBR analysis, the amount of rod bow is taken into account by applying a DNBR penalty; therefore it does not contribute to the enthalpy rise engineering hot channel factor.

3. Inlet flow mal-distribution

Studies performed on 1/7-scale hydraulic reactor models indicate that a conservative design basis is to consider a 5% reduction in the flow to the hot fuel assembly under isothermal conditions. The effect of this inlet flow reduction increases the hot channel enthalpy rise by approximately 1%.

4. Flow redistribution

This is considered in the sub-channel analysis code (VIPRE-01) by inherently including boiling and flow redistribution effects. Therefore, this does not contribute to the enthalpy rise engineering hot channel factor.

## **5. Flow mixing**

Mixing vanes, in 400 and 422 VANTAGE+ grids, are incorporated into the spacer grid design to induce flow mixing between the various flow channels in a fuel assembly and also between adjacent assemblies. This mixing reduces the enthalpy rise in the hot channel resulting from local power peaking or unfavorable mechanical tolerances. These effects are considered in the sub-channel analysis code (VIPRE-01) by using a conservative thermal diffusion coefficient determined from sub-channel mixing tests.

### **Pressure Drop and Hydraulic Forces**

The total pressure loss across the reactor vessel, including the inlet and outlet nozzles, and the pressure drop across the core are listed in Table 3.2-1. These values include a 10% uncertainty factor. The hydraulic forces are not sufficient to lift a control rod cluster during normal operation even if the rod is not attached to its coupling. The pressure drop across the 400 and 422 VANTAGE+ fuel assembly hot channel is also shown in Table 3.2-1.

### **Thermal and Hydraulic Parameters**

The thermal and hydraulic design parameters are given in Table 3.2-1.

### **Effects of DNB on Neighboring Rods**

DNB has never been observed to occur in a group of neighboring rods in a rod bundle as a result of DNB in one rod in the bundle.

### **DNB with Physical Burnout**

Westinghouse (Reference 76) has conducted DNB tests in a 25-rod bundle where physical burnout occurred with one rod. After this occurrence, the 25-rod test section was used for several days to obtain more DNB data from the other rods in the bundle. The burnout and deformation of the rod did not affect the performance of neighboring rods in the test section during the burnout or the validity of the subsequent data points. No occurrences of flow instability or other abnormal operation were observed.

### **DNB with Return to Nucleate Boiling**

Additional DNB tests have been conducted by Westinghouse (Reference 77) in 19 and 21-rod bundles. In these tests, DNB without physical burnout was experienced more than once on single rods in the bundles for short periods of time. Each time, a reduction to power of approximately 10% was sufficient to re-establish nucleate boiling on the surface of the rod.

During these and subsequent tests, no adverse effects were observed on this rod or any other rod in the bundle as consequences of operating in DNB.

## Hydrodynamic and Flow Power Coupled Instability

Boiling flows may be susceptible to thermohydrodynamic instabilities (Ref. 78). These instabilities are undesirable in reactors since they may cause a change in thermo-hydraulic conditions that may lead to a reduction in the DNB heat flux relative to that observed during a steady-flow condition or to undesired forced vibrations of core components. Therefore, a thermohydraulic design criterion was developed which states that modes of operation under Conditions I and II events shall not lead to thermohydrodynamic instabilities.

Two specific types of flow instabilities are considered for Westinghouse PWR operation. These are the Ledinegg or flow excursion type of static instability, and the density wave type of dynamic instability.

A Ledinegg instability involves a sudden change in flow rate from one steady-state to another. This instability occurs (Ref. 78) when the slope of the RCS pressure drop-flow rate curve  $\frac{\partial \Delta P}{\partial G_{\text{internal}}}$  becomes algebraically smaller than the loop supply (pump head)

pressure drop-flow rate curve  $\frac{\partial \Delta P}{\partial G_{\text{external}}}$ . The criterion for stability is thus

$\frac{\partial \Delta P}{\partial G_{\text{internal}}} > \frac{\partial \Delta P}{\partial G_{\text{external}}}$ . The Westinghouse pump head curve has a negative slope

( $\partial \Delta P / \partial G_{\text{external}} < 0$ ), whereas the Reactor Coolant System pressure drop-flow curve has a positive slope ( $\partial \Delta P / \partial G_{\text{internal}} > 0$ ) over the Conditions I and II operational ranges. Thus, a Ledinegg instability will not occur.

The mechanism of density wave oscillations in a heated channel has been described by Labey and Moody (Ref. 79). Briefly, an inlet flow fluctuation produces an enthalpy perturbation. This perturbs the length and the pressure drop of the single-phase region and causes quality or void perturbations in the two-phase regions which travel up the channel with the flow. The quality and length perturbations in the two-phase region create two-phase pressure drop perturbations. However, since the total pressure drop across the core is maintained by the characteristics of the fluid system external to the core, then the two-phase pressure drop perturbation feeds back to the single phase region. These resulting perturbations can be either attenuated or self-sustained.

A simple method has been developed by Ishii (Ref. 80) for parallel closed channel systems to evaluate whether a given condition is stable with respect to the density wave type of dynamic instability. This method had been used to assess the stability of typical Westinghouse reactor designs (Ref. 81, 82 and 83), including Virgil C. Summer, under Conditions I and II operation. The results indicate that a large margin-to-density wave instability exists (e.g., increases on the order of 200 percent of rated reactor power would be required for the predicted inception of this type of instability).

The application of the method of Ishii (Ref. 80) to Westinghouse reactor designs is conservative due to the parallel open channel feature of Westinghouse PWR cores. For such cores, there is little resistance to lateral flow leaving the flow channels of high power density. There is also energy transfer from channels of high power density to lower power density channels. This coupling with cooler channels has led to the opinion that an open channel configuration is more stable than the above closed channel analysis under the same boundary conditions. Flow stability tests (Ref. 83) have been conducted where the closed channel systems were shown to be less stable than when the same channels were cross-connected at several locations. The cross connections were such that the resistance to channel-to-channel cross flow and enthalpy perturbations would be greater than that which would exist in a PWR core which has a relatively low resistance to cross flow.

Flow instabilities which have been observed have occurred almost exclusively in closed channel systems operating at low pressures relative to the Westinghouse PWR operating pressures. Kao, Morgan and Parker (Ref. 85) analyzed parallel closed channel stability experiments simulating a reactor core flow. These experiments were conducted at pressures up to 2,200 psia. The results showed that for flow and power levels typical of power reactor conditions, no flow oscillations could be induced above 1,200 psia.

Additional evidence that flow instabilities do not adversely affect thermal margin is provided by the data from the rod bundle DNB tests. Many Westinghouse rod bundles have been tested over wide ranges of operating conditions with no evidence of premature DNB or inconsistent data which might be indicative of flow instabilities in the rod bundle.

In summary, it is concluded that thermohydrodynamic instabilities will not occur under Conditions I and II modes of operation for Westinghouse PWR reactor designs. A large power margin, greater than doubling-rated power, exists to predicted inception of such instabilities. Analysis has been performed which shows that minor plant-to-plant differences in Westinghouse reactor designs such as fuel assembly arrays, core power flow ratios, fuel assembly length, etc., will not result in gross deterioration of the above power margins.

**3.2.2.4 Effect of Fuel Rod Bow on Thermal Hydraulic Performance****3.2.2.4.1 Rod Bow As Applied to DNBR Analysis**

DNBR reduction as a result of rod bow is calculated by:

$$\text{MDNBR}_B = \text{MDNBR}_{NB} (1 - \delta_B)$$

where

MDNBR = minimum DNBR

MDNBR<sub>NB</sub> = MDNBR for nonbowed fuel

MDNBR<sub>B</sub> = MDNBR for bowed fuel

$\delta_B$  = rod bow penalty, fractional reduction in MDNBR due to bowing

Westinghouse's detailed methodology for calculating fuel rod bowing and its MDNBR effect is given in Reference 61.

$\delta_B$  is given as a function of assembly average burnup. The value of  $\delta_B$  is 0.030 and 0.029 for 400 and 422 VANTAGE +, respectively for low flow. These values bound the full flow value of the rod bow penalty and are used for the full and reduced flow calculations. These rod bow penalties are representative for an assembly average burnup of 24,000 MWD/MTU (Reference 68).

While the amount of rod bowing increases beyond this exposure, the fuel is not capable of achieving limiting peaking factors due to the decrease in fissionable isotopes and the buildup of fission product inventory. The physical burndown effect is greater than the rod bowing effects which would be calculated based on the amount of bow predicted at those burnups.

Therefore, for the purpose of evaluating effects of rod bow on Westinghouse fuel, 24,000 MWD/MTU represents the maximum burnup of concern.

The reduction in MDNBR is accounted for by taking a DNBR penalty for all Condition I and II events where the penalty applies.

**3.2.2.4.2 Effect of Rod Bow on LOCA Limits**

The Prairie Island Plant Technical Specification incorporates a total nuclear peaking augmentation factor of 1.0815 in calculation of the ECCS safety limits which includes a 1.03 engineering subfactor, and a 1.05 subfactor for measurement uncertainty. This factor is adequate to accommodate nuclear augmentation due to rod bow for burnups up to the middle of life (24,000 MWD/MTU, Reference 68). Fuel assemblies with exposures in excess of this will be operating below the LOCA limits due to the reduction of assembly reactivity. Therefore, no additional penalty due to rod bow needs to be applied to calculation of LOCA limits.

The total nuclear peaking augmentation is calculated from the following equation:

$$F_{Q}^{U} = 1.0 + (\sigma_{E}^2 + \sigma_{M}^2 + \sigma_{B}^2)^{1/2}$$

where

$F_{Q}^{U}$  = total nuclear peaking augmentation factor

$\sigma_{E}$  = fractional augmentation due to engineering subfactor = 3% (pellet density, diameter, enrichment)

$\sigma_{M}$  = nuclear measurement uncertainty = 5%

$\sigma_{B}$  = nuclear augmentation due to rod bow

In order for the total peaking augmentation factor to be below 1.0815, the nuclear augmentation due to rod bow must be 5.7% or less. Current fuel has been shown to have nuclear augmentation due to rod bow factors equal to or less than 5.7% (Reference 89).

**THIS PAGE IS LEFT INTENTIONALLY BLANK**



### **3.3 NUCLEAR CHARACTERISTICS**

This section presents the nuclear characteristics of the core and an evaluation of the characteristics and design parameters which are significant to design objectives. The capability of the reactor to achieve these objectives while performing safely under operational modes, including both transient and steady state, is described.

#### **3.3.1 Design Basis**

The nuclear design bases for the core are as follows:

- a. The design shall permit operation within the Technical Specifications of the Prairie Island plants.
- b. The end of cycle exposure for each cycle is such that all fuel pins in the cycle remain within the exposure limits for the given fuel type.
- c. The loading pattern shall be designed to achieve power distribution constraints given in Section 3.2.1 and control rod reactivity worth constraints such that the scram worth of all rods minus the most reactive shall exceed shutdown margin requirements at any time during a fuel cycle.
- d. The core shall have a negative power coefficient.
- e. The isothermal temperature coefficient shall be less than +5 pcm/°F for power operation up to 70% of full power and negative or less than 0 pcm/°F from 70% to 100% full power at all times during power operation.

The neutronic design methods utilized to ensure the above requirements are consistent with those described in Section 14.3.

#### **3.3.2 Nuclear Design Data**

##### **3.3.2.1 Reactivity Control Aspects**

Reactivity control is provided by 1) a soluble chemical neutron absorber in the reactor coolant (boric acid, also called chem shim), 2) movable neutron absorbing control rods, and 3) burnable poison in the form of gadolinium oxide dispersed in uranium dioxide matrix.

The concentration of boric acid is varied as necessary during the life of the core to compensate for: (1) changes in reactivity which occur with change in temperature of the reactor coolant from Mode 5, Cold Shutdown to Mode 2, Startup, zero power conditions; (2) changes in reactivity associated with changes in the fission product poisons xenon and samarium; (3) reactivity losses associated with the depletion of fissile inventory and buildup of long-lived fission product poisons (other than xenon and samarium); (4) changes in reactivity due to burnable poison burnup; (5) load-follow operation; and (6) reactivity changes associated with the power coefficient.

The control rods provide reactivity control for: (1) fast shutdown; and (2) reactivity changes listed for boric acid. The control rods are divided into two categories according to their function. The rods which compensate for changes in reactivity due to variations in operating conditions of the reactor, such as power or temperature, comprise the control group of rods. The other rods provide additional shutdown reactivity and are termed shutdown rods. The total shutdown worth of all the rods is specified to provide adequate shutdown with the most reactive rod stuck out of the core.

### **3.3.2.2 Kinetic Characteristics**

The response of the reactor core to plant conditions or operator adjustments during normal operation, as well as the response during abnormal or operational transients, is evaluated by means of a detailed plant simulation. In these calculations, reactivity coefficients are required to couple the response of the core neutron multiplication to the variables which are set by conditions external to the core. Since the reactivity coefficients change during the life of the core, a range of coefficients is established to determine the response of the plant throughout life and to establish the design of the Reactor Control and Protection System.

#### **3.3.2.2.1 Moderator Temperature Coefficient of Reactivity**

The safety analysis uses the best estimate moderator temperature coefficient plus or minus a reliability factor or the Technical Specification limit to ensure conservative results. Moderator temperature coefficient is an inferred parameter determined by subtracting the predicted fuel temperature coefficient from an experimentally determined isothermal temperature coefficient which is measured directly during startup physics testing. This isothermal temperature coefficient is defined as the reactivity change associated with a unit change in the moderator and fuel temperatures. Essentially it is then the sum of the moderator and fuel temperature coefficients.

The moderator temperature coefficient becomes more positive or less negative as the concentration of boric acid is increased. For extended cycle length it is necessary to either load the reactor with burnable poisons and/or increase the boron concentration in the reactor coolant system. If the boron concentration is increased, then it is possible that the isothermal temperature coefficient could be slightly positive at low power.

**3.3.2.2.2 Moderator Pressure Coefficient of Reactivity**

The moderator pressure coefficient is positive at plant operating conditions. Its effect on core reactivity and stability is small because of the small magnitude of the pressure coefficient, a change of 50 psi in pressure having no more effect on reactivity than a half-degree change in moderator temperature.

**3.3.2.2.3 Doppler Coefficient of Reactivity**

The Doppler coefficient is defined as the change in neutron multiplication per degree change in fuel temperature. The coefficient is obtained by calculating neutron multiplication as a function of effective fuel temperature.

**3.3.2.3 Summary of Control Rod Requirements****3.3.2.3.1 Total Power Reactivity Defect**

Control rods must be available to compensate for the reactivity changes associated with rapid power decreases. As power is decreased positive reactivity is added by the power reactivity defect, primarily due to the doppler and moderator coefficients. Control rods must have sufficient negative reactivity to control the plant under these conditions. The power reactivity defect is largest at end of life, therefore, the largest requirement for control rods occurs at end of life.

**3.3.2.3.2 Control Rod Bite**

For good plant performance (e.g., response to rapid changes in load) the controlling group of absorber rods are normally positioned to maintain a minimum value of reactivity insertion rate. The partial control rod insertion to achieve this is called control rod bite.

**3.3.2.3.3 Excess Reactivity Insertion Upon Reactor Trip**

The control requirements are nominally based on providing one percent shutdown at hot, zero power conditions with the highest worth rod stuck in its fully withdrawn position, or to prevent return to an unacceptable high power level following a credible steam-line break, whichever is the more limiting.

### **3.3.3 Nuclear Design Evaluation**

#### **3.3.3.1 Physics Characteristics**

The calculated reactivity coefficients of the current Unit 1 and 2 cores are bounded by the coefficients used in the safety analysis (Section 14.4). The effect of the gadolinia is reflected in the calculations.

#### **3.3.3.2 Power Distribution Considerations**

The control of the core power distribution is accomplished by following criteria as outlined in Technical Specifications Sections 3.1 and 3.2. Reference 69 provides the means for projecting the maximum  $F_Q(z)$  variation anticipated during operation. This bounding variation in  $F_Q(z)$  represents the maximum variation when the flux difference,  $\Delta I$ , is maintained within the range defined in the Core Operating Limits Report, COLR.

#### **3.3.3.3 Control Rod Reactivity Requirements**

Shutdown margin is calculated by the methods referenced in Section 14.3.

#### **3.3.3.4 Isothermal Temperature Coefficient Considerations**

The Technical Specifications require that the isothermal temperature coefficient be negative above 70% power and less than 5pcm/°F at or below 70% power.

#### **3.3.3.5 Utilization of Gadolinia as a Burnable Poison**

The core loadings may include fresh fuel assemblies with gadolinia bearing ( $\text{UO}_2 - \text{Gd}_2\text{O}_3$ ) pins. The core loading pattern is designed to achieve a desirable power distribution while reducing the beginning of cycle (BOC) boron concentration.

The effect of the gadolinia poison is calculated per the methods referenced in Section 14.3.

#### **3.3.3.6 Analytical Methodology**

The methods used in the core analysis are consistent with those described in Section 14.3.

**3.3.4 DELETED****3.3.4.1 DELETED****3.3.4.2 Dynamic Rod Worth Measurement Technique**

Westinghouse Dynamic Rod Worth Measurement (DRWM) technique (Reference 71) is one method of measuring the reactivity worth of individual control and shutdown banks control rod worth during physics testing after refueling. It is a fast process (relative to dilution or rod swap) that is accomplished by inserting and withdrawing the bank at the maximum stepping speed, without changing boron concentration, and recording the signals on the excore detectors. The recorded signals are processed on the reactivity computer, which solves the inverse point kinetics equation with proper analytical compensation for spatial effects. DRWM has been reviewed and approved by the NRC for measurement of rod worth at the beginning of reload cycles for two, three, and four loop Westinghouse cores (Reference 72).

DRWM was developed by Westinghouse as an improved method of measuring rod worth. DRWM has several advantages over other measurement techniques;

- The worth of all banks are measured individually. Only one bank of rods is in the core at any given time; thus the worth of the bank in the core is determined without the other control banks being present.
- The integral rod worth as a function of position is determined for every bank, providing more data to validate the design calculation models used in the safety analysis.
- The technique is much simpler for plant operations personnel to perform, reducing the possibility of human error.
- The technique can save several hours of critical path time during startup.

A summary of the DRWM technique is as follows:

1. With the rods in a fully withdrawn position, insert the test bank in a continuous motion until it is fully inserted and then withdraw it.
2. While the flux is recovering, adjust the signals recorded during the insertion for static special effects.
3. Calculate reactivity using the inverse point kinetics equations to analyze the adjusted flux signals.
4. Adjust the calculated reactivity for dynamic spatial effects. Continue the test with the next bank of rods.

01448624

01448624

**THIS PAGE IS LEFT INTENTIONALLY BLANK**

### **3.4 FUEL MECHANICAL CHARACTERISTICS**

#### **3.4.1 Design Basis**

The fuel assemblies are designed to perform satisfactorily throughout their lifetime. The loads, stresses, and strains resulting from the combined effects of flow induced vibrations, earthquakes, reactor pressure, fission gas pressure, fuel growth, thermal strain, and differential expansion during both steady state and transient reactor operating conditions have been considered in the design of the fuel rods and fuel assembly. The assembly is also structurally designed to withstand handling and shipping loads prior to irradiation, and to maintain sufficient integrity at the completion of design burnup to permit safe removal from the core and subsequent handling during cooldown, shipment, storage and fuel reprocessing.

The fuel rods are supported at several locations along their length within the fuel assemblies by brazed (for the Inconel grid) or welded (for the Zircaloy or ZIRLO straps) grid assemblies which are designed to maintain control of the lateral spacing between the rods throughout the design life of the assemblies. The magnitude of the support loads provided by the grids are established to minimize possible fretting without overstressing the cladding at the points of contact between the grids and fuel rods. The grid assemblies also allow axial thermal expansion of the fuel rods without imposing restraint of sufficient magnitude to result in buckling or distortion of the rods. The fuel rod cladding is designed to withstand operating pressure loads without collapse or rupture and to maintain encapsulation of the fuel throughout the design life.

The specific design criteria for reload fuel are as follows:

- a. The fuel assemblies shall be mechanically compatible with the reactor core, steam supply system, fuel handling tools and system, existing fuel, control rods, burnable poison rods, and thimble plugging devices.
- b. The reload fuel shall be compatible with the existing fuel assemblies on the basis of coolant flow and neutronic characteristics.
- c. The fuel shall be designed to prevent a Departure from Nucleate Boiling at design overpower conditions.
- d. The fuel assemblies shall be designed to minimize the peak cladding temperature following a postulated loss of coolant accident (LOCA) consistent with current licensing criteria.

### **3.4.2 Description of Fuel Assemblies**

#### **3.4.2.1 Fuel Assembly**

The fuel assemblies for Prairie Island are arranged in a 14x14 square array of 179 fuel rods with 16 control rod guide tubes, and one (1) instrumentation tube.

The fuel rod cladding is cold worked and stress relieved ZIRLO or partially re-crystallized annealed Optimized ZIRLO. Each standard fuel rod contains a column of enriched  $\text{UO}_2$  fuel pellets with an enriched  $\text{UO}_2$  annular blanket at each end. The pellets are pressed and sintered to 95% theoretical density, and are dished on both ends. Gadolinia bearing fuel rods, when part of the fuel assembly design, contain  $\text{UO}_2\text{-Gd}_2\text{O}_3$  fuel pellets.

The fuel rod upper plenum contains a stainless steel compression spring to prevent fuel column separation during fabrication and shipping. The end caps are Zircaloy. End caps are seal welded to the cladding during fuel rod assembly. Fuel rods are pressurized with helium to provide a good heat transfer medium.

The fuel rods are supported at intervals along their length by Zircaloy/ZIRLO and Inconel-718 grids. The top and bottom grids are fabricated from Inconel-718 while the five mid grids are fabricated from Zircaloy or ZIRLO. These grids maintain the lateral spacing between the rods. The spacers are axially positioned so that the thermal hydraulic performance will be compatible with existing fuel assemblies. Each guide tube has a reduced diameter on the lower end to provide dashpot damping for the control rods. The guide tubes are mechanically attached to the upper and lower nozzles.

The upper nozzle assembly is a machined stainless steel casting which has four (4) Inconel 718 holddown spring assemblies. These springs are attached to the nozzle by clamps and cap screws. The lower nozzle assembly is a machined stainless steel casting. The spacers, guide tubes, and nozzles form the structural framework of the fuel assembly.

The fuel rods are axially positioned with the upper and lower end caps approximately equidistant from the upper and lower nozzles. Axial fuel rod growth is allowed for by the clearance between the fuel rod end caps and nozzles. The upper nozzle assembly can be mechanically removed and reinstalled on a fuel assembly (under water in a fuel pool) to allow inspection of irradiated fuel rods and the capability to replace a fuel rod.

01284359

01454730

01284359

01284359



### **3.4.2.2 Fuel Rods**

The fuel assemblies contain an enriched column of  $\text{UO}_2$  or  $\text{UO}_2\text{-Gd}_2\text{O}_3$  with annular  $\text{UO}_2$  pellets on each end of the enriched  $\text{UO}_2$  column. The gadolinia burnable poison rod assemblies have  $\text{Gd}_2\text{O}_3$  dispersed in the  $\text{UO}_2$  matrix. The gadolinia fuel rods provide the advantages of permitting longer fuel cycles and higher batch discharge exposures, permitting shaping of the radial power distribution, and increasing the flexibility of fuel management schemes. The upper plenum contains a stainless steel spring. The rods are purged and prepressurized with helium, and Zircaloy end caps are fusion welded to the cladding.

The mechanical design analysis for the burnable poison rods is enveloped by the analysis for the standard fuel rods. The enrichment in these rods is reduced so that temperatures, stresses and strains in the poison rods are not limiting.

See Table 3.1-1 for details of fuel rods and pellets.

### **3.4.2.3 Nozzles**

The upper nozzle assembly is the upper structural component of the fuel assembly and locates the upper end of the assembly relative to the upper reactor core plate. The upper nozzle assembly is a box structure and a holddown spring system. The holddown spring system is four (4) sets of double leaf springs designed to apply sufficient holddown force to ensure that the fuel assembly does not lift off during normal operation and anticipated transients, other than the hot pump overspeed transient. Effects of fuel assembly growth and spring force reduction, due to permanent set and irradiation-induced stress relaxation, are considered. Double leaf springs give more deflection capability without yielding than is possible with a single leaf design. This extra spring compliance makes the spring design less sensitive to dimensional tolerance stackups. All upper nozzle assembly parts, with the exception of the springs are type 304 stainless steel. The springs are Inconel Alloy 718.

The lower nozzle is type 304 stainless steel. This nozzle controls the coolant flow to the fuel assembly and functions as the bottom structural component for the fuel assembly.

### **3.4.2.4 Guide Tube**

The guide tubes are fabricated from ZIRLO tubing. The guide tubes are fuel assembly structural members and also provided channels for either control rods, burnable absorbers or thimble plugs.

The guide tubing consists of two diameters. The larger diameter along most of the length permits rapid insertion of the control rods during a reactor trip. The lower portion below the second grid from the bottom has a reduced diameter that produces a dashpot action near the end of the control rod travel during a reactor trip. This decelerates the control rod and reduces the impact forces between the control rod spider hub and fuel assembly upper tie plate at the end of travel. Orifice holes are provided in the tube wall to allow water to exit, thus controlling the rod drop time.

#### **3.4.2.5 Grid Spacers**

The fuel rods are laterally supported at intervals along their length by grid assemblies which maintain the lateral spacing between the rods. Each fuel rod is given support at six contact points within each grid cell by a combination of support dimples and springs. The grid assembly consists of individual interlocking slotted straps that are joined by brazing for the Inconel grid or welding for the Zircaloy/ZIRLO straps.

The top and bottom grid material is Inconel 718, which provides corrosion resistance, high strength properties and resistance to irradiation-induced stress relaxation. The five mid grids are fabricated from Zircaloy or ZIRLO which provides good neutron economy properties. The magnitude of the grid restraining force on the fuel rod is designed to minimize fretting without overstressing the cladding at the points of contact between the grids and fuel rods. The grid assemblies also allow axial thermal expansion and irradiation-induced growth of the fuel rods while imposing minimal axial restraining forces on the fuel rods.

The outside straps of all grids contain guide vanes and guide tabs which, in addition to their mixing function, aid in guiding the fuel assemblies past adjacent surfaces during handling.

#### **3.4.2.6 Fuel Assembly Overall Structure**

The overall Westinghouse fuel assembly design for both the 400 and 422 VANTAGE + fuel is described in Reference 89.

### **3.4.3 Design Evaluation**

#### **3.4.3.1 Rod Design Evaluation**

##### **3.4.3.1.1 External Cladding Corrosion**

For Unit 1, the cladding oxidation limits are given in Reference 96. For Unit 2, the clad surface temperature (oxide-to-metal interface) shall not exceed those clad temperature limits required to preclude a condition of accelerated clad oxidation as given in References 65 and 66.

01284359 01284359

01454730

### **3.4.3.1.2 Cladding Hydrogen Absorption**

Clad hydrogen pickup limits are required to prevent excessive degradation of clad mechanical properties due to hydrogen embrittlement by the formation of zirconium hydride platelets when hydrogen is released during the clad oxidation reaction. The clad end-of-life hydrogen pickup limit has been set at 600 ppm to preclude any loss of ductility due to hydrogen embrittlement consistent with references 65, 66 (Unit 2) and reference 96 (Unit 1).

Extended burnup operation for the VANTAGE+ fuel affects clad hydriding primarily due to the higher power operation in later cycles for the VANTAGE+ fuel. Data have shown (References 66 and 68) that ZIRLO and Zircaloy hydriding have essentially the same relationship to oxidation, i.e., the clad hydriding behavior is characterized by a constant fractional hydrogen pickup relative to the theoretical maximum, as a function of oxide thickness. The reduced corrosion of the ZIRLO tubing is more than sufficient to compensate for the effects of the more limiting VANTAGE+ fuel duty on the ZIRLO clad hydriding levels for lead rod burnups up to 75,000 MWD/MTU. Optimized ZIRLO has superior corrosion performance compared to ZIRLO and the resulting hydrogen content in the rods will be reduced correspondingly (Reference 91).

### **3.4.3.1.3 Stress Corrosion Cracking**

#### **a. Iodine Concentration**

The possibility that the combination of volatile fission products and high cladding stresses may lead to stress corrosion cracking has been recognized for some time. Quantitative data are available (References 27 through 30) which indicates that the probability of failure is a function of fission product concentration at the inside cladding surface, stress level, strain rate and tubing texture.

Stress corrosion cracking of fuel rod cladding is considered the principal failure mechanism for the pellet-cladding interaction (PCI) failures that are encountered during changes in reactor operating conditions (References 28 and 30). Even though unanimous agreement has not been reached on which chemical species enhances failure, the iodine atmosphere is usually considered the primary attacking agent for irradiated fuel. The iodine concentration and cladding strain rate are significant in determining the ultimate ductility of the cladding; but, if the stress level is low enough in the cladding, then stress corrosion cracking does not occur. Tests have been performed under EPRI support (Reference 30) to evaluate the iodine stress threshold. Figures 3.4-1 and 3.4-2 show typical data from this program. The time dependence of stress corrosion rupture is primarily controlled by two processes. The high stress process is represented by the steep slope portion of Figure 3.4-2 and is controlled by the crack propagation process. The lower stress process is represented by the shallow slope portion of Figure 3.4-2 and is controlled by a time dependent crack nucleation process.

01454730

01284359

01454730

Stress corrosion cracking tests (References 28, 30) have shown that an iodine concentration greater than  $10^{-5}$  to  $10^{-6}$  g/cm<sup>2</sup> is needed to activate the stress corrosion cracking process at normal inside cladding temperatures between 300 and 400°C. It is believed that these concentrations can never be reached under steady-state conditions due to recombination of free iodine. Reference 29 indicates that the highest sensitivity to low ductility stress corrosion failure is for strain rates between  $10^{-3}$  to  $10^{-4}$ /hr. Thus, stress corrosion cracking may only be active under transient reactor operating conditions.

b. Texture

Stress corrosion cracks in metals preferentially initiate and propagate along specific crystallographic planes. The preferred crystallographic direction for stress corrosion cracks in zircaloy is along a plane at an angle of approximately 15° with the basal plane. Work by Peels, et. al. (Reference 28) has shown that grains with basal pole directions between 0° and 50° with the surface have a diminished tendency to crack in an iodine atmosphere. Similarly, work carried out by the Stanford Research Institute has shown that zircaloy tubing with a higher frequency of basal poles in the radial direction of the tube has a higher iodine stress corrosion cracking threshold than tubing with more tangentially directed poles.

The crystallographic texture of zircaloy tubing in the radial direction is commonly characterized by the quantitative texture number  $f_r$  which is derived from a direct or an inverse pole figure. In integral form,  $f_r$  is given by:

$$f_r = \int_0^{\pi/2} [I_\varnothing] \sin \varnothing \cos^2 \varnothing d\varnothing$$

where  $I_\varnothing$  is the average pole density at an angle  $\varnothing$  from the reference direction. The value of  $f_r$  can vary between 0 and 1 indicating perfect alignment of basal poles perpendicular and parallel to the radial direction respectively. From this definition of  $f_r$  and the foregoing, it is evident that tubing with a high  $f_r$  value is less susceptible to stress corrosion cracking than tubing with a low  $f_r$  value.

Measurement of the contractile strain ratio or R-value has been shown to be a method to determine the texture number  $f_r$  (Reference 31). For tubing deformed in tension in the axial direction the R-value is defined as the differential of the true plastic circumferential strain ( $\epsilon_r^P$ ) with respect to the true plastic radial or thickness strain ( $\epsilon_\varnothing^P$ ), i.e.

$$R = \frac{d\epsilon_r^P}{d\epsilon_\varnothing^P}$$

The contractile strain ratio is determined using the plastic wall thickness strain ( $\epsilon_r$ ) for a tube subject to an axial plastic tensile strain of 2%. The relation between the texture number and the R-value is given by:

$$f_r = \frac{R}{R + 1}$$

For most zircaloy tubing, R can vary from approximately 1.00 to 1.85 which corresponds to a variation in  $f_r$  between 0.50 and 0.65. Measurement of the R-value can be a method to evaluate stress corrosion susceptibility. A high R-value indicates lower susceptibility and a low R-value indicates higher susceptibility to stress corrosion attack.

c. Strain Limits

The design limit for fuel rod cladding strain during steady-state operation is that the total plastic tensile creep and uniform cylindrical fuel pellet expansion due to fuel swelling and thermal expansion shall not exceed 1% from the unirradiated condition. This criterion addresses slow-strain rate mechanisms where the clad effective stress never reaches the yield strength of the material due to stress relaxation.

During steady-state operation tensile clad creep strain results primarily from cladding stresses caused by pellet swelling and thermal expansion following the closing of the pellet-clad gap. Since rod power levels and hence fuel temperature, decrease as a function of burnup, the fuel pellet diameter increase at extended burnup caused by the fuel swelling effect is somewhat mitigated by the reduced thermal expansion. Evaluation of clad strain during steady-state operation is performed using the PAD code (Reference 87).

For transients, the design limit for cladding strain is that the total tensile strain due to uniform cylindrical pellet thermal expansion during the transient shall be less than 1% from the pretransient value. The present 1% limit on circumferential strain is based upon the results of tensile and high stress rate biaxial tests on irradiated tubing. These limits are consistent with proven practice.

For transients, analyses have shown the tensile creep strains, resulting from pellet thermal expansion, are most limiting at the end of the second cycle of operation when transient clad stress is most limiting. Results also show that transient strain criteria, and therefore transient strain limits are always met when transient stress limits are met. These evaluations are performed using the PAD code (Reference 87).

d. Cladding Internal Surface

A rough cladding inside surface finish significantly increases the loads required to insert a column of pellets and increases the probability of pellet cracking and chipping which may contribute toward fuel failures.

Pellet-cladding interaction (PCI) that leads to fuel rod failure has been identified as primarily due to stress corrosion cracking of the cladding. Tests to evaluate SCC cracking in two batches of zircaloy tubing, manufactured to the same specifications by two suppliers, have shown significant differences in susceptibility to SCC (Reference 25). When the internal surface of the more susceptible tubing was polished, the susceptibility decreased dramatically. Other research proposes that SCC crack initiation is increased in cladding with inside surface flaws by one or a combination of the following mechanisms:

1. Easier or more frequent breakdown of ID surface oxide film due to surface flaws.
2. Locally increased stress or change of stress ratio.
3. Ease of the crack initiation process through localized chemical differences.
4. Removal of favorable surface texture.

The surface condition requirements were selected based upon SCC considerations and tubing manufacturing capabilities.

#### **3.4.3.1.4 Cladding Stress and Strain During Steady-State Operation**

Tests (References 26, 32 through 41) on irradiated tubing indicate failure at relatively low mean strains. The test results for tensile, burst, and split ring tests show a ductility between 1.2% and 5% at normal reactor operating temperatures.

The presence of iodine or other fission products can cause the cladding to fail at lower strain levels. However, susceptibility to this type of failure (stress corrosion cracking) occurs only when the fission product concentration is high, the strain rate is between  $10^{-4}$  and  $10^{-3}$ /hr, and the stress is above a threshold value. As pointed out in Section 3.4.3.1.3 above, all of these conditions are unlikely under steady-state or near steady-state operation. Thus, creep and burst tests on irradiated cladding in a non-corrosive atmosphere can establish ductility limits since these failures are usually associated with unstable or localized regions of high deformation after some uniform deformation.

To prevent cladding failure due to plastic instability and localized strain, design criteria limit the steady-state cladding circumferential plastic strain to 1.0% at EOL and the maximum clad stress intensities either:

- (1) less than the 0.2% offset yield stress with due consideration to temperature and irradiation effects under Condition I and II modes of operation (References 65 and 91),  
  
or
- (2) excluding pellet cladding interaction but accounting for cladding corrosion as a loss of load carrying metal, to less than the limits defined in Reference 88, based on the ASME calculations.

01494866

#### **3.4.3.1.5 Fatigue Damage**

Cyclic mechanical strains can cause cumulative damage and subsequent failure which may be predicted by fatigue analysis techniques. O'Donnell and Langer (Reference 42) have developed a zircaloy fatigue analysis design curve which is presented in Figure 3.4-3. This curve is based on fatigue test data with a margin of 2 on stress or 10 on number of cycles, whichever is the most conservative.

The design limit for clad strain fatigue is that the fatigue life usage factor is less than 1.0. That is, for a given strain range the number of strain fatigue cycles are less than those required for failure, considering a minimum safety factor of 2 on the stress amplitude or a minimum safety factor of 20 on the number of cycles, whichever is more conservative.

The evaluation of the fatigue life usage factor for extended burnup design conservatively assumes daily load follow operation over the life of the fuel rod. The PAD code (Reference 87). is used to determine the strain range for the fatigue life usage analysis. The Langer-O'Donnell strain fatigue model (Reference 42) with experimentally determined correlation coefficients from Westinghouse testing programs is used in the fatigue evaluation. The conservative assumption of daily load follow operation is assumed to be a typical ramp pattern described as a reference "12-3-6-3" daily load cycle. The plant runs at full power for 12 hours, ramps down to the lower power level over three hours, maintains the lower power level for six hours and ramps back to full power in three hours. The power level changes for a load cycle are conservatively assumed to be from 100% full power to 15% of full power. The fatigue performance of ZIRLO and Optimized ZIRLO cladding have been confirmed through testing. Testing of unirradiated Optimized ZIRLO cladding shows that Optimized ZIRLO has the same fatigue performance as ZIRLO cladding (Reference 91).

01284359

#### **3.4.3.1.6 Creep Collapse**

If significant gaps form in the pellet column due to fuel densification, the pressure differential between the inside and outside of the cladding can act to increase the cladding ovality. Ovality increase by clad creep to the point of plastic instability would result in collapse of the cladding (a flattened area) in the region of the pellet column gap.

Although many collapsed rods from other vendors have operated successfully in reactors, there have been a few failures attributed to collapse. The increase in peaking and postulated reduction in thermal margins has resulted in operating restrictions for some plants.

Through proper design, the probability of creep collapse can be significantly reduced. Typical pellets are relatively dimensionally stable. Fuel densification as determined by the fuel pellet fabrication parameters, e.g., density and sintering temperature, is verified as part of the standard cycle-specific fuel rod design, using the region-specific as-fabricated fuel pellet characteristics, to ensure stable pellets during irradiation (Reference 66).

Plenum spring is included in the fuel rod design to prevent formation of gaps in the pellet column **during transportation only**. The fuel rods are helium prepressurized to prevent creep collapse if a pellet column gap were present. This is the minimum prepressurization, based upon the conservative COLLAP evaluation, which will prevent creep collapse.

#### **3.4.3.1.7 Fuel Rod Internal Pressure**

The fuel rod internal pressure is primarily a function of the initial fuel rod pressurization, fuel swelling, and fission gas release. The minimum fuel rod fill pressure is set at a level designed to prevent creep collapse (Section 3.4.3.1.6) and to assure acceptable thermal performance of the fuel. Post-irradiation measurements have demonstrated that significant fission gas release can occur in LWR fuels when rod powers exceed a threshold level. This release can be greatly magnified by the fission gas release thermal feedback effect. Magnification of fission gas release can be virtually eliminated if the initial helium pressurization is high enough so that when fission gas release does occur, it does not produce a significant reduction in gas conductance across the pellet-to-cladding gap. The maximum fill pressure is designed so that in combination with the fission gas release, the fuel rod end-of-life pressure does not cause the pellet-to-cladding gap to reopen (Reference 67).



---

**3.4.3.1.8 Fuel Rod and Guide Tube Growth**

Axial extension of the fuel rods results from both irradiation growth and pellet to cladding interaction. Excessive axial extension of fuel rods can interfere with the tie plates and result in significant rod bow. Excessive axial extension of guide tubes could result in solid contact with the reactor core plates and possibly cause fuel assembly bow.

The irradiation growth rate for 78% cold worked, lightly stress relieved zircaloy tubing is substantially greater than for annealed tubing (Reference 43). At higher burnups, PCI stresses and the resulting ratcheting can also increase the fuel rod growth rate. ZIRLO and Optimized ZIRLO clad fuel rods have reduced fuel rod axial extension compared to Zircaloy clad fuel rods (References 65 and 91).

01284359

A fuel assembly must have sufficient axial clearance between the tie plates and fuel rods to account for the maximum anticipated difference between fuel rod growth and guide tube growth at EOL.

Design calculations assure that the fuel assembly length after guide tube growth does not exceed the reactor core plate to core plate spacing.

**3.4.3.1.9 Creep Bow**

Fuel rod bow is determined throughout the life of the fuel assembly so that reactor operating thermal limits can be established. These limits include the minimum DNB associated with protection against the potential fuel rod burnout, as well as the maximum allowable fuel rod linear heat generation rate (LHGR) associated with protection against exceeding the allowable peak cladding temperature for a postulated loss-of-coolant accident. This is discussed further in Section 3.2.2.4.

**3.4.4 Surveillance and Testing**

Each month the plant nuclear engineering staff evaluates the core performance for each unit. Included in the evaluation is a review of iodine concentration, iodine ratios, gas activity and beta gamma activity. The data obtained is compared to historical data so that trends and/or abnormalities can be identified.

**THIS PAGE IS LEFT INTENTIONALLY BLANK**

### **3.5 REACTIVITY CONTROL MECHANICAL CHARACTERISTICS**

#### **3.5.1 Design Basis**

The control system and the operational procedures provide adequate control of the core reactivity and power distribution. The following control limits are met:

- a. Sufficient control is available to produce a hot shutdown margin of at least 1% delta k/k.
- b. The shutdown margin is maintained with the most reactive RCCA stuck in the fully withdrawn position.
- c. The shutdown margin is maintained at ambient temperature by the use of soluble poison.

#### **3.5.2 Control Methods**

Reactivity is added at a prescribed and controlled rate in bringing the reactor from a shutdown condition to a low power level during startup by RCCA withdrawal. Although the initial startup procedure uses the method of boron dilution, the normal startup is with RCCA withdrawal. RCCA motion can cause much faster changes in reactivity than can be made by changing boron concentration.

##### **3.5.2.1 Rod Cluster Control Assemblies**

The control rods or rod cluster control (RCC) assemblies each consist of a group of individual absorber rods fastened at the top end to a common hub or spider assembly. These assemblies, one of which is shown in Figure 3.1-3 are provided to control the reactivity of the core under operating conditions.

The absorber material used in the control rods is a silver-indium-cadmium alloy in the form of extruded rods, which is essentially “black” to thermal neutrons and has sufficient additional resonance absorption to significantly increase its worth. The absorber material is sealed in stainless steel to prevent the rods from coming in direct contact with the coolant.

The overall control rod length is such that when the assembly has been withdrawn through its full travel, the tip of the absorber rods remains engaged in the guide thimbles so that alignment between rods and thimbles is always maintained. Since the rods are long and slender, they are relatively free to conform to any small misalignments with the guide thimble.

The spider assembly is in the form of a center hub with radial vanes containing cylindrical fingers from which the absorber rods are suspended. Handling detents, and detents for connection to the drive shaft, are machined into the upper end of the hub. A spring pack is assembled into a skirt integral to the bottom of the hub to stop the RCC assembly and absorb the impact energy at the end of a trip insertion. The radial vanes are joined to the hub, and the fingers are joined to the vanes by furnace brazing. A centerpost which holds the spring pack and its retainer is threaded into the hub within the skirt and welded to prevent loosening in service.

All components of the spider assembly are made from Type 304 stainless steel except for the springs which are Inconel X-750 alloy and the retainer which is of 17-4 PH materials.

The absorber rods are secured to the spider so as to assure trouble free service. The rods are first threaded into the spider fingers and then pinned to maintain joint tightness, after which the pins are welded in place. The end plug below the pin position is designed with a reduced section to permit flexing of the rods to correct for small operating or assembly misalignments.

In construction, the silver-indium-cadmium rods are inserted into cold-worked stainless steel tubing which is then sealed at the bottom and the top by welded end plugs. Sufficient diametral and end clearance are provided to accommodate relative thermal expansions and to limit the internal pressure to acceptable levels.

The criteria used for the design of the cladding on the individual absorber rods in the rod cluster control assemblies (RCCA) are similar to those used for the fuel rod cladding. The stainless steel cladding is designed to be free standing under all operating conditions and will maintain encapsulation of the absorber material throughout the absorber rod design life. Allowance for wear during operation is not included in the RCCA cladding thickness, but the newer RCCAs also have a wear resistant chrome plating on the cladding.

Adequate clearance is provided between the absorber rods and the guide thimbles which position the rods within the fuel assemblies so that coolant flow along the length of the absorber rods is sufficient to remove the heat generated without overheating of the absorber cladding. The clearance is also sufficient to compensate for any misalignment between the absorber rods and guide thimbles and to prevent mechanical interference between the rods and guide thimbles under any operating conditions.

Stainless steel clad silver-indium-cadmium alloy absorber rods are resistant to radiation and thermal damage thereby ensuring their effectiveness under all operating conditions.

The bottom plugs are made bullet-nosed to reduce the hydraulic drag during a reactor trip and to guide smoothly into the dashpot section of the fuel assembly guide thimbles. The upper plug is threaded for assembly to the spider and has a reduced end section to make the joint more flexible.

### **3.5.2.2 Neutron Source Assemblies**

No neutron source assemblies are currently being used.

### **3.5.2.3 Plugging Devices**

Plugging devices were used to limit bypass flow through the RCC guide thimbles. An analysis has shown that the difference in bypass flow with and without plugging devices was insignificant. Therefore, the plugging devices were removed from the core for cycle 11 of both units.

The safety evaluation for this modification is contained in "Prairie Island Unit 1 and 2, Safety Evaluation for RCC Guide Thimble Plug Removal", NSPNAD-8412, April 1985 (Reference 54). While this modification was performed under 10 CFR 50.59, the NRC did express interest in reviewing the NSP safety evaluation regarding the thimble plug removal. The NRC documented their review in a safety evaluation that was transmitted by letter from Edward J. Butcher (USNRC) to D M Musolf (NSP), dated October 18, 1985 (Reference 55).

## **3.5.3 Control Rod Drive System**

### **3.5.3.1 Rate of Response**

The control rod drive assemblies provide rod cluster control assembly insertion and withdrawal rates consistent with the required reactivity changes for reactor operational load changes. This rate is based on the worths of the various rod groups, which are established to limit power peaking flux patterns to design values. The maximum reactivity addition rate is specified to limit the magnitude of a possible nuclear excursion resulting from a control system malfunction or operator error.

Also, the control rod drive assemblies provide a fast insertion rate during a "trip" of the RCC assemblies which results in a rapid shutdown of the reactor for conditions that cannot be handled by the reactor control system. This rate is input to the various reactor transient analyses (Section 14), taking into account instrument and control delay times and the amount of reactivity that must be inserted before deceleration of the RCC assembly occurs, to assure that acceptable results are obtained in terms of preventing rupture of the reactor coolant pressure boundary or disrupting the core or vessel internals to a degree so as to lose capability to cool the core.

### **3.5.3.2 Control Rod Drive Mechanism**

#### **3.5.3.2.1 General Description**

Each control rod drive assembly is designed as a hermetically sealed unit to prevent leakage of reactor coolant water. All pressure-containing components are designed to meet the requirements of the ASME Code, Section III, Nuclear Vessels for Class 1 vessels.

The magnetic latch control rod drive mechanisms are used for withdrawal and insertion of the full-length rod cluster control assemblies into the reactor core and to provide sufficient holding power for stationary support.

Fast total insertion (reactor trip) is obtained by simply removing the electrical power allowing the rods to fall by gravity.

The complete drive mechanism, shown in Figure 3.5-1, consists of the internal (latch) assembly, the pressure vessel, the operating coil stack, the drive shaft assembly, and the position indicator coil stack.

Each assembly is an independent unit which can be dismantled or assembled separately. Each drive is welded to an adaptor on top of the reactor pressure vessel and is connected to the control rod (directly below) by means of a grooved drive shaft. The upper section of the drive shaft is suspended from the working components of the drive mechanism. The drive shaft and control rod remain connected during reactor operation, including tripping of the rods.

Reactor coolant fills the pressure containing parts of the drive mechanism. All working components and the shaft are immersed in the coolant.

Three magnetic coils, which form a removable electrical unit and surround the rod drive pressure housing induce magnetic flux through the housing wall to operate the working components. They move two sets of latches which lift or lower the grooved drive shaft.

The three magnets are turned on and off in a fixed sequence by solid-state switches for the full length rod assemblies.

The sequencing of the magnets produces step motion over the 144 inches of normal control rod travel.

The mechanism develops a minimum lifting force of three times the static load of a control rod. Therefore, extra lift capacity is available for overcoming mechanical friction between the moving and the stationary parts. Gravity provides the drive force for rod insertion and the weight of the whole rod assembly is available to overcome any resistance.

01047869

01047869

The mechanisms are designed to operate in water at 650°F and 2485 psig. The temperature at the mechanism head adaptor will be much less than 650°F because it is located in a region where there is limited flow of water from the reactor core, while the pressure is the same as in the reactor pressure vessel.

A multi-conductor cable connects the mechanism operating coils to the 125 volt d-c power supply. The power supply is described in Section 8.

a. Latch Assembly

The latch assembly contains the working components which withdraw and insert the drive shaft and attached control rod. It is located within the pressure housing and consists of the pole pieces for three electromagnets. They actuate two sets of latches which engage the grooved section of the drive shaft.

The upper set of latches moves up or down to raise or lower the drive rod by 5/8 inch. The lower set of latches has a maximum 1/16 inch axial movement to shift the weight of the control rod from one set of latches to the other. In the de-energized condition, the latch assembly does not engage the drive shaft.

b. Pressure Vessel

The pressure vessel consists of the latch housing and rod travel housing. The latch housing is the lower portion of the vessel and contains the latch assembly. The rod travel housing is the upper portion of the vessel. It provides space for the drive shaft during its upward movement as the control rod is withdrawn from the core.

The housings are designed in accordance with the requirements of Section III, Division 1, Subsection NB, Class 1, ASME B & PVC Code.

c. Operating Coil Stack

The operating coil stack is an independent unit which is installed on the drive mechanism by sliding it over the outside of the pressure housing. It rests on a pressure housing flange without any mechanical attachment and can be removed or installed while the reactor is pressurized.

The operator coils (A, B and C) are made of round copper wire which is insulated with a double layer of filament type glass yarn.

01047869

01047869

Each of the 29 control rod drive mechanism (CRDM) operating coils has a heat dissipation of 12 kw. The coils are cooled by forced-flow ventilation system. Two integral vaneaxial fans, with automatically controlled discharge shutoff dampers draw air from containment. Each fan is capable of handling 100% of the system requirements; i.e., 13,000 cfm. The fans take a suction from a common duct with turning vanes drawing containment air through the cooling coils discharging through a damper to the plenum. The plenum supplies four internal ducts that discharge air downward to the center of the lower CRDM shroud inside the CRDM grid, below the CRDM coil stacks. This forced air cooling along the outside of the coil stack maintains a coil temperature of less than 392°F.

A visual and audible annunciator alarms in the control room for any improper status of the CRDM cooling system and equipment.

In the unlikely event that the design operating temperatures of the control rod drive mechanism coils were to be exceeded, over a period of time, the life of the coil would be degraded and hence the plant would be shutdown to avoid coil damage. Failure of one coil would at most result in the dropping of a single rod into the core.

Failure of a CRDM coil will not affect rod position determining capability.

d. Drive Shaft Assembly

The main function of the drive shaft is to connect the control rod to the mechanism latches. Grooves for engagement and lifting by the latches are located throughout the 144 in. of control rod travel. The grooves are spaced 5/8 inch apart to coincide with the mechanism step length and have 45° angle sides.

The drive shaft is attached to the control rod by the coupling. The coupling has two flexible arms which engage the grooves in the spider assembly.

A 1/4 inch diameter disconnect rod runs down the inside of the drive shaft. It utilizes a locking button at its lower end to lock the coupling and control rod. At its upper end, there is a disconnect assembly for remote disconnection of the drive shaft assembly from the control rod. During reactor operation, the drive shaft assembly remains connected to the RCC assembly.

e. Position Indicator Coil Stack

The position indicator coil stack slides over the rod travel housing section of the pressure vessel. It detects drive rod position by means of cylindrically wound differential transformers which span the normal length of the rod travel (144 inches).



**f. Drive Mechanism Materials**

All parts exposed to reactor coolant, such as the pressure vessel, latch assembly and drive rod, are made of metals which resist the corrosive action of the water.

Three types of metals are used exclusively: stainless steels, Inconel X, and cobalt based alloys. Wherever magnetic flux is carried by pressure containing parts exposed to the main coolant, stainless steel is used. Cobalt based alloys are used for the pins and latch tips.

Inconel X is used for the springs of both latch assemblies and 316 stainless steel is used for all pressure containing parts. Hard chrome plating provides wear surfaces on the sliding parts and prevents galling between mating parts (such as threads) during assembly.

Outside of the pressure vessel, where the metals are exposed only to the reactor plant containment environment and cannot contaminate the main coolant, carbon and stainless steels are used. Carbon steel, because of its high permeability, is used for flux return paths around the operating coils. It is zinc-plated 0.001 inch thick to prevent corrosion.

**3.5.3.2.2 Principles of Operation**

The drive mechanisms shown schematically in Figure 3.5-2 withdraw and insert their respective control rods as electrical pulses are received by the operator coils.

ON and OFF sequence, repeated by solid state switches in the power programmer causes either withdrawal or insertion of the control rod. Position of the control rod is indicated by the differential transformer action of the position indicator coil stack surrounding the rod travel housing. The differential transformer output changes as the top of the ferromagnetic drive shaft assembly moves up the rod travel housing.

Generally, during plant operation, the drive mechanisms hold the control rods withdrawn from the core in a static position, and only the stationary gripper coil is energized on each mechanism.

**Control Rod Withdrawal:** The control rod is withdrawn by repeating the following sequence:

**a. Movable Gripper Coil - ON**

The movable gripper armature rises and swings the movable gripper latches into the drive shaft groove.

b. Stationary Gripper Coil - OFF

Gravity causes the stationary gripper latches and armature to move downward until the load of the drive shaft is transferred to the movable gripper latches. Simultaneously, the stationary gripper latches swing out of the shaft groove.

c. Lift Coil - ON

The gap between the lift armature and the lift magnet pole closes and the drive rod rises one step length (5/8 inch).

d. Stationary Gripper Coil - ON

The stationary gripper armature rises and closes the gap below the stationary gripper armature, and swings the stationary gripper latches into a drive shaft groove. The latches contact the shaft and lift it a maximum 1/16 inch. The load is so transferred from the movable to the stationary gripper latches.

e. Movable Gripper Coil - OFF

The movable gripper armature separates from the lift armature under the force of a spring and gravity. Three links, pinned to the movable gripper armature, swing the three movable gripper latches out of the groove.

f. Lift Coil - OFF

The gap between the lift armature and the lift magnet pole opens. The movable gripper latches drop 5/8 inch to a position adjacent to the next groove.

Control Rod Insertion: The sequence for control rod insertion is similar to that for control rod withdrawal:

a. Lift Coil - ON

The movable gripper latches are raised to a position adjacent to a shaft groove.

b. Movable Gripper Coil - ON

The movable gripper armature rises and swings the movable gripper latches into a groove.

c. Stationary Gripper Coil - OFF

The stationary gripper armature moves downward and swings the stationary gripper latches out of the groove.

- d. Lift Coil - OFF

Gravity separates the lift armature from the lift magnet pole and the control rod drops down 5/8 inch.

- e. Stationary Gripper Coil - ON

- f. Movable Gripper Coil - OFF

The sequences described above are termed as one step or one cycle and the control rod moves 5/8 inch for each cycle. Each sequence can be repeated at a rate of up to 72 steps per minute and the control rods can therefore be withdrawn or inserted at a rate of up to 45 inches per minute. No credible mechanical or electrical control system malfunction can cause a rod cluster to be withdrawn at a speed greater than 72 steps per minute.

#### Control Rod Tripping:

If power to the gripper coils is cut off, as for tripping, the combined weight of the drive shaft and the rod cluster control assembly is sufficient to move the latches out of the shaft groove. The control rod falls by gravity into the core. The tripping occurs as the magnetic field, holding the gripper armatures against the lift magnet, collapses and the gripper armatures are forced down by the weight acting upon the latches.

### **3.5.4 Operation and Performance Analysis**

#### **3.5.4.1 CRDM Housing Mechanical Failure Evaluation**

##### **3.5.4.1.1 General**

An evaluation of the possibility of damage to adjacent control rod drive mechanism housings in the event of a circumferential or longitudinal failure of a rod housing located on the vessel head is presented. This Westinghouse evaluation, which is not specific to Prairie Island, was inserted at the end of a section in the original submittal Final Safety Analysis Report and, thus, was evaluated by the U.S. Atomic Energy Commission Directorate of Licensing in its safety evaluation of the plant.

The operating coil stack assembly of this mechanism has a 10.8 inch by 10.8 inch cross section and a 39.875 inch length. The position indicator coil stack assembly is located above the operating coil stack assembly. It surrounds the rod travel housing over nearly its entire length. The rod travel housing outside diameter is 3.8 inches and the position indicator coil stack assembly consists of a 1/8" thick stainless steel tube surrounded by a continuous stack of copper wire coils. This assembly is held together by two end plates (the top end plate is square), an outer sleeve, and four axial tie rods.

**3.5.4.1.2 Effect of Rod Travel Housing Longitudinal Failures**

Should a longitudinal failure of the rod travel housing occur, the region of the stainless steel tube opposite the break would be stressed by the reactor coolant pressure of 2250 psia. The most probable leakage path would be provided by the radial deformation of the position indicator coil assembly, resulting in the growth of axial flow passages between the rod travel housing and the stainless steel tube. A radial free water jet is not expected to occur because of the small clearance between the stainless steel tube and the rod travel housing, and the considerable resistance of the combination of the stainless steel tube and the position indicator coils to internal pressure. Calculations based on the mechanical properties of stainless steel and copper at reactor operating temperature show that an internal pressure of at least 4000 psia would be necessary for the combination of the stainless steel tube and the coils to rupture.

Therefore, the combination of stainless steel tube and copper coils stack is more than adequate to prevent formation of a radial jet following a control rod housing split which assures the integrity of the adjacent rod housings.

**3.5.4.1.3 Effect of Rod Travel Housing Circumferential Failures**

If circumferential failure of a rod travel housing should occur, the broken-off section of the housing would be ejected vertically because the driving force is vertical and the position indicator coil stack assembly and the drive shaft would tend to guide the broken-off piece upwards during its travel. Travel is limited by the missile shield, thereby limiting the projectile acceleration. When the projectile reaches the missile shield, it would partially penetrate the shield and dissipate its kinetic energy. The water jet from the break would push the broken-off piece against the missile shield.

If the broken-off piece were short enough to clear the break when fully ejected, it could rebound after impact with the missile shield. The top end plates of the position indicator coil stack assemblies would prevent the broken piece from directly hitting the rod travel housing of a second drive mechanism. Even if a direct hit by the rebounding piece were to occur, the low kinetic energy of the rebounding projectile would not be expected to cause significant damage.

**3.5.4.1.4 Summary**

The considerations given above lead to the conclusion that failure of a control rod housing due to either longitudinal or circumferential cracking would not cause damage to adjacent housings that would increase the severity of the initial accident.

**3.5.4.2    RCCA Cladding Wear**

In June 1983 cladding wear was observed during a Point Beach refueling shutdown. Some of the wear observed was due to contact between the guide plate surfaces (in the guide tubes) and the RCCA rodlets. In order to reduce this wear at Prairie Island for those rods normally fully withdrawn, these RCCAs will not always be withdrawn to the same position. Fully withdrawn is normally 228 steps. However, 225 steps was evaluated and found not to be significantly different neutronically to the core or analytically to the safety analysis. Therefore, fully withdrawn rods will be withdrawn to a position between 228 and 225 steps inclusive.

**3.5.4.3    Multiple Control Rod Drop Times**

During rod drop testing, most utilities normally drop a single rod to determine rod drop time; however, several utilities using Westinghouse designs have gathered rod drop data during multiple rod drops. Data gathered from these sites for the multiple rod drops are consistent with that for single rod drops and are within the same sigma limits.

**THIS PAGE IS LEFT INTENTIONALLY BLANK**

### **3.6 OTHER REACTOR VESSEL INTERNALS**

#### **3.6.1 Design Basis**

##### **Mechanical Limits**

The reactor internal components are designed to withstand the stresses resulting from startup, steady state operation with any number of pumps running, and shutdown conditions. No damage to the reactor internals occurs as a result of loss of pumping power.

Lateral deflection and torsional rotation of the lower end of the core barrel are limited to prevent excessive movements resulting from seismic disturbances and thus prevent interference with RCC assemblies. Core drop in the event of failure of the normal supports is limited so that the rod cluster control assemblies do not disengage from the fuel assembly guide thimbles (Reference 44).

The structural internals are designed to maintain their functional integrity in the event of a loss-of-coolant accident. The dynamic loading resulting from the pressure oscillations because of a loss-of-coolant accident does not prevent rod cluster control assembly insertion even during an earthquake.

The reactor internals are designed to support and orient the reactor core fuel assemblies and RCCA, absorb the control rod dynamic loads and transmit these and other loads to the reactor vessel flange, provide a passageway for the reactor coolant, and support incore instrumentation. The reactor internals are shown in Figure 3.1-2.

The internals are designed to withstand the forces due to weight, preload of fuel assemblies, control rod dynamic loading, vibration, possible blowdown forces, and earthquake acceleration. Under the loading conditions, including conservative effects of design earthquake loading, the structure satisfies stress values prescribed in Section III, ASME Nuclear Vessel Code (Reference 44). The dynamic criteria for design and stress levels of the internals are described in Section 12.2.1.5.2.2.1.

The reactor internals are equipped with bottom-mounted incore instrumentation supports. These supports are designed to sustain the applicable loads outlined above.

In the event of downward vertical displacement of the internals, energy absorbing devices limit the displacement by contacting the vessel bottom head. The load is transferred through the energy absorbing devices to the vessel. The energy absorbers, cylindrical in shape, are contoured on their bottom surface to the reactor vessel bottom head geometry. Their number and design are determined so as to limit the forces imposed to a safe fraction of yield strength. Assuming a downward vertical displacement, the potential energy of the system is absorbed mostly by the strain energy of the energy absorbing devices. See Figure 3.6-1.

The free fall in the hot condition is on the order of 1/2 inch, and there is an additional strain displacement in the energy absorbing devices of approximately 3/4 inch. Alignment features in the internals prevent locking of the internals structure during this postulated drop. The control system as designed provides assurance of control rod insertion capabilities under these assumed drop conditions. The drop distance of about 1-1/4 inch is not enough to cause the tips of the shutdown group of RCC assemblies to come out of the guide tubes in the fuel assemblies.

### **3.6.2 Description**

The components of the reactor internals are divided into three parts consisting of the lower core support structure (including the entire core barrel and thermal shield), the upper core support structure and the incore instrumentation support structure.

#### **3.6.2.1 Lower Core Support Structure**

The major containment and support member of the reactor internals is the lower core support structure, shown in Figure 3.6-1. This support structure assembly consists of the core barrel, the core baffle, the lower core plate and support columns, the thermal shield, the intermediate diffuser plate and the bottom support plate which is welded to the core barrel. All the major material for this structure is Type 304 Stainless Steel. The core support structure is supported at its upper flange from a ledge in the reactor vessel head flange and its lower end is restrained in its transverse movement by a radial support system attached to the vessel wall. Within the core barrel are axial baffle and former plates which are attached to the core barrel wall and form the enclosure periphery of the assembled core. The lower core plate is positioned at the bottom level of the core below the baffle plates and provides support and orientation for the fuel assemblies.

The lower core plate provides the necessary flow distributor holes for each fuel assembly. Fuel assembly locating pins (two for each assembly) are also inserted into this plate. Columns are placed between this plate and the bottom support plate of the core barrel in order to provide stiffness to this plate and transmit the core load to the bottom support plate. Intermediate between the support plate and lower core support plate is positioned a perforated plate to diffuse uniformly the coolant flowing into the core.



Irradiation baskets in which materials samples can be inserted and irradiated during reactor operation are attached to the thermal shield. The irradiation capsule basket supports are welded to the thermal shield. There is no extension of this support above the thermal shield as was done in the older designs. Thus, the basket has been removed from the high flow disturbance zone. The welded attachment to the shield extends the full length of the support except for small interruptions about one inch long. This type of attachment has an extremely high natural frequency. The specimens are held in position within the baskets by a stop on the bottom and a slotted cylindrical spring at the top which fits against a relief in the basket. The specimen does not extend through the top of the basket and thus is protected by the basket from the flow. Refer to Section 4.7 for further details.

The lower core support structure and principally the core barrel serve to provide passageways and control for the coolant flow. Inlet coolant flow from the vessel inlet nozzles proceeds down the annulus between the core barrel and the vessel wall, flows on both sides of the thermal shield, and then into a plenum at the bottom of the vessel. It then turns and flows up through the lower support plate, passes through the intermediate diffuser plate and then through the lower core plate. The flow holes in the diffuser plate and the lower core plate are arranged to give a very uniform entrance flow distribution to the core. After passing through the core the coolant enters the area of the upper support structure and then flows generally radially to the core barrel outlet nozzles and directly through the vessel outlet nozzles.

A small amount of water flows between the baffle plates and core barrel to provide additional cooling of the barrel. Similarly, a small amount of the entering flow is directed into the vessel head plenum and exits through the vessel outlet nozzles.

Vertically downward loads from weight, fuel assembly preload, control rod dynamic loading and earthquake acceleration are carried by the lower core plate partially into the lower core plate support flange on the core barrel shell and partially through the lower support columns to the bottom support plate and thence through the core barrel shell to the core barrel flange supported by the vessel head flange. Transverse loads from earthquake acceleration, coolant cross flow, and vibration are carried by the core barrel shell to be shared by the lower radial support to the vessel head flange. Transverse acceleration of the fuel assemblies is transmitted to the core barrel shell by direct connection of the lower core support plate to the barrel wall and by a radial support type connection of the upper core plate to slab sided pins pressed into the core barrel.

The main radial support system of the core barrel is accomplished by "key" and "keyway" joints to the reactor vessel wall. At equally spaced points around the circumference, an Inconel block is welded to the vessel I.D. Another Inconel block is bolted to each of these blocks, and has a "keyway" geometry. Opposite each of these is a "key" which is attached to the internals. At assembly, as the internals are lowered into the vessel, the keys engage the keyways in the axial direction. With this design, the internals are provided with a support at the farthest extremity, and may be viewed as a beam fixed at the top and simply supported at the bottom.

Radial and axial expansions of the core barrel are accommodated but transverse movement of the core barrel is restricted by this design. With this system, cycle stresses in the internal structures are within the ASME Section III limits.

### **3.6.2.2 Upper Core Support Assembly**

The upper core support assembly, shown in Figure 3.6-2, consists of the upper support plate and upper core plate between which are support columns and guide tube assemblies. The support columns which establish the spacing between the upper support plate and the upper core plate are fastened at top and bottom to these plates. The support columns transmit the mechanical loadings between the two plates and serve the supplementary function of supporting thermocouples and guide tubes. The guide tube assemblies, shown on Figure 3.6-3, sheath and guide the control rod drive shafts and control rods and provide no other mechanical functions. They are fastened to the upper support plate and are guided by pins in the upper core plate for proper orientation and support. Additional guidance for the control rod drive shafts is provided by the upper guide tube which is bolted to the upper support plate and guide tube.

Due to anticipated problems with guide tube support pins, the original upper core support assemblies were replaced in both units at the end of Cycle 10. The replacement upper core support assemblies are an improved design which includes an improved guide tube design with an improved support pin design, a simplified fully-machined upper support assembly with fewer parts and weld joints, a refined support column design, elimination of flow mixers, and a thicker upper core plate. A safety evaluation addressing the replacement upper core support assembly design (Reference 60) was submitted for the information of the NRC Staff prior to their installation.

The upper core support assembly, which is removed as a unit during refueling operation, is positioned in its proper orientation with respect to the lower support structure by flat-sided pins pressed into the core barrel which in turn engage in slots in the upper core plate. At an elevation in the core barrel where the upper core plate is positioned, the flat-sided pins are located at equal angular positions. Slots are milled into inserts in the upper core plate at the same positions. As the upper support structure is lowered into the main internals, the inserts in the plate engage the flat-sided pins in the axial direction. Lateral displacement of the plate and of the upper support assembly is restricted by this design. Fuel assembly locating pins protrude from the bottom of the upper core plate and engage the fuel assemblies as the upper assembly is lowered into place. Proper alignment of the lower core support structure, the upper core support assembly, the fuel assemblies and control rods is thereby assured by this system of locating pins and guidance arrangement. The upper core support assembly is restrained from any axial movements by a large circumferential spring which rests between the upper barrel flange and the upper support plate flange and is compressed by the reactor vessel head flange/studs.

Vertical loads from fuel assembly preload are transmitted through the upper core plate via the support columns to the upper support plate flange and then through the circumferential spring to the reactor vessel head. Transverse loads from coolant cross flow, earthquake acceleration, and possible vibrations are distributed by the support columns to the top support plate and upper core plate. The top support plate is particularly stiff to minimize deflection.

### **3.6.2.3 Incore Instrumentation Support Structures**

The incore instrumentation support structures consist of an upper system to convey and support thermocouples penetrating the vessel through the head and a lower system to convey and support flux thimbles penetrating the vessel through the bottom.

The upper system utilizes the reactor vessel head penetrations. Instrumentation port columns are slip-connected to in-line columns that are in turn fastened to the upper support plate. These port columns protrude through the head penetrations. The thermocouples are routed through these port columns and across the upper support plate to positions above their readout locations. The thermocouple conduits are supported from the columns of the upper core support system. The thermocouple conduits are sealed stainless steel tubes.

In addition to the upper incore instrumentation, there are reactor vessel bottom port columns which carry the retractable, cold worked stainless steel flux thimbles that are pushed upward into the reactor core. Conduits extend from the bottom of the reactor vessel down through the concrete shield area and up to a thimble seal line. The minimum bend radii are about 90 inches and the trailing ends of the thimbles (at the seal line) are extracted approximately 13 feet during refueling of the reactor in order to avoid interference within the core. The thimbles are closed at the leading ends and serve as the pressure barrier between the reactor pressurized water and the nuclear detector.

Mechanical seals between the retractable thimbles and the surrounding conduits are provided to seal the reactor coolant from the containment atmosphere. Thus primary system pressure exists up to the seal table. During normal operation, the retractable thimbles are stationary in the core and move only during refueling or for maintenance, at which time a space of approximately 13 feet above the seal table is cleared for the retraction. Section 7.6 contains more information on the layout of the incore instrumentation system.

The incore instrumentation support structure is designed for adequate support of instrumentation during reactor operation and is rugged enough to resist damage or distortion under the conditions imposed by handling during the refueling sequence.

### **3.6.3 Performance Analysis**

The internals design is based on analysis, test and operational information. Substantial scale model testing was performed by Westinghouse. This included tests which involved a complete full scale fuel assembly which was operated at reactor flow, temperature and pressure conditions. Tests were run on a 1/7th scale model of the Indian Point reactor. Measurements taken from these tests indicate very little shield movement, on the order of a few mils when scaled up to actual size. Strain gage measurements taken on the core barrel also indicate very low stresses. Testing to determine thermal shield excitation due to inlet flow disturbances have been included. Information gathered from these tests was used in the design of the thermal shield and core barrel. It can be concluded from the testing program and the analyses with the experience gained that the design as employed here is adequate. In WCAP-7718 "Westinghouse PWR Internals Vibration Summary" Westinghouse experience and results are reported.

The response of the reactor core and vessel internals under excitation produced by a simultaneous complete severance of a reactor coolant pipe and seismic excitation for typical 2-loop plant internals has been determined. A detailed description of the analysis applicable to the Prairie Island design, appears in Reference 44, 56, 57, 58 and 59.

The following subsections discuss analyses based on the rupture of the large loop piping. As discussed in Sections 4.6.2.3 and 4.6.2.4, Prairie Island has approval to use leak before break (LBB) for the large primary loop piping and the Unit 1 pressurizer surge line piping. Using LBB eliminates the need to evaluate the effects from ruptures in these lines on the reactor internals (i.e., dynamic effects). However, the effects on the reactor internals from a postulated rupture of the other piping which connects to the RCS still needs to be considered. In general, the mass flow and acoustic pressure effects from a rupture of the larger loop piping are more limiting than rupture of a smaller branch line.

#### **3.6.3.1 Reactor Internals Response Under Blowdown and Seismic Excitation**

A loss-of-coolant accident may result from a rupture of reactor coolant piping. During the blowdown of the coolant, critical components of the core are subjected to vertical and horizontal excitation as a result of rarefaction waves propagating inside the reactor vessel.

For these large breaks, the reduction in water density greatly reduces the reactivity of the core, thereby shutting down the core whether the rods are tripped or not. (The subsequent refilling of the core by the Emergency Core Cooling System uses borated water to maintain the core in a subcritical state.) Therefore, the main requirement is to assure effectiveness of the Emergency Core Cooling System. Insertion of the control rods, although not needed, gives further assurance of ability to shut the plant down and keep it in a safe shutdown condition.

The pressure waves generated within the reactor are highly dependent on the location and nature of the postulated pipe failure. In general, the more rapid the severance of the pipe, the more severe the imposed loadings on the components. A one millisecond severance time is taken as the limiting case in all cases except the analysis of the baffle barrel bolting.

In the case of the hot leg break, the vertical hydraulic forces produce an initial upward lift of the core. A rarefaction wave propagates through the reactor hot leg nozzle into the interior of the upper core barrel. Since the wave has not reached the flow annulus on the outside of the barrel, the upper barrel is subjected to an impulsive compressive wave. Thus, dynamic instability (buckling) or large deflections of the upper core barrel or both is the possible response of the barrel during hot leg blowdown. In addition to the above effects, the hot leg break results in transverse loading on the upper core components as the fluid exits the hot leg nozzle.

In the case of the cold leg break, a rarefaction wave propagates along a reactor inlet pipe arriving first at the core barrel at the inlet nozzle of the broken loop. The upper barrel is then subjected to a nonaxisymmetric expansion radial impulse which changes as the rarefaction wave propagates both around the barrel and down the outer flow annulus between vessel and barrel. After the cold leg break, the initial steady-state hydraulic lift forces (upward) decrease rapidly (within a few milliseconds) and then increase in the downward direction. These cause the reactor core and lower support structure to move initially downward.

If a simultaneous seismic event with the intensity of the design basis earthquake (DBE) is postulated with the loss-of-coolant accident, the imposed loading on the internals component may be additive in certain cases and therefore the combined loading must be considered. The replacement upper internals, however, were designed combining the blowdown loads and earthquake loads by square root sum of the squares. In general, however, the loading imposed by the earthquake is small compared to the blowdown loading and can generally be ignored.

### **3.6.3.2 Acceptance Criteria for Results of Analyses**

The criteria for acceptability in regard to mechanical integrity analysis is that adequate core cooling and core shutdown must be assured. This implies that the deformation of the reactor internals must be sufficiently small so that the geometry remains substantially intact. Consequently, the limitations established on the internals are concerned principally with the maximum allowable deflections and/or stability of the parts in addition to a stress criterion to assure integrity of the components.

**3.6.3.2.1 Allowable Deflection and Stability Criteria****Upper Barrel**

The upper barrel deformation has the following limits:

- a. To insure a shutdown and cooldown of the core during blowdown, the basic requirement is a limitation on the outward deflection of the barrel at the locations of the inlet nozzles connected to the unbroken lines. A large outward deflection of the barrel in front of the inlet nozzles, accompanied with permanent strains, could close the inlet area and stop the cooling water coming from the accumulators. Consequently, a permanent barrel deflection in front of the unbroken inlet nozzles larger than a certain limit, called the "no-loss of function" limit, could impair the efficiency of the Emergency Core Cooling System.
- b. To assure rod insertion and to avoid disturbing the Control Rod Cluster guide structure, the barrel should not interfere with the guide tubes. This condition also requires a stability check to assure that the barrel will not buckle under the accident loads.

**Control Rod Cluster Guide Tubes**

The guide tubes in the upper core support package house the control rods. The deflection limits were established from tests.

**Fuel Assembly**

The limitations for this case are related to the stability of the thimbles in the upper end. The upper end of the thimbles must not experience stresses above the allowable dynamic compressive stresses. Any buckling of the upper end of the thimbles due to axial compression could distort the guide line and thereby affect the free fall of the control rod.

**Upper Package**

The local vertical deformation of the upper core plate, where a guide tube is located, shall be below 0.100 inch. This deformation will cause the plate to contact the guide tube since the clearance between plate and guide tube is 0.100 inch. This limit will prevent the guide tubes from undergoing compression. For a plate local deformation of 0.150 inch, the guide tube will be compressed and deformed transversely to the upper limit previously established; consequently, the value of 0.150 inch is adopted as the no loss of function local deformation, with an allowable limit of 0.100 inch.

**3.6.3.2.2 Allowable Stress Criteria**

For this faulted condition the allowable stress criteria using elastic or inelastic methods of analysis are given by Table 3.6-1. Plastic analysis acceptance criteria in ASME Section III Non-mandatory Appendix F, paragraph F-1340, 1998 Edition with Addenda through 2000 may also be used. This table defines various criteria based upon their corresponding method of analysis. To account for multi-axial stresses, the von Mises theory is also considered.

**3.6.3.3 Method of Analysis**

As stated in the LAR (Reference 93), the LOCA hydraulic forces analysis for the reactor vessel and internals were generated using the advanced beam model version of MULTIFLEX (3.0) (Reference 94) assuming a conservative break opening time of 1 msec; in accordance with the methodology accepted by the NRC in WCAP-15029 (Reference 95). This version of the MULTIFLEX code shares a common hydraulic modeling scheme with the NRC-approved MULTIFLEX (1.0) computer code with the differences being confined to a more realistic downcomer hydraulic network and a more realistic core barrel structural model that accounts for nonlinear boundary conditions and vessel motion. Generally, this improved modeling results in more realistic, but still conservative, hydraulic forces on the core barrel.

The MULTIFLEX computer code calculated the thermal-hydraulic transient within the RCS and considers subcooled, transition, and early two-phase blowdown regimes. Limitations to the use of the WCAP-15029 methodology as stated in the associated NRC SER were applied. The LATFORC and FORCE2 post-processing codes were then used to generate the LOCA forces on the component of interest from the thermal-hydraulic data calculated from the MULTIFLEX code.

WCAP-15029-P-A provides the option of employing a break-opening time larger than the 1 millisecond. The justification for increased break-opening times is based upon information provided in WCAP-14748 Rev.0, "Justification for Increasing Postulated Break Opening Times in Westinghouse Pressurizer Water Reactor". WCAP-14748 Rev. 0 was reviewed by the NRC in an associated safety evaluation (SER). The WCAP-14748 SER states that the future application to other issues involving different phenomena outside of baffle barrel bolting program will require the staff's review on a case-by-case basis. The NRC staff found the use of WCAP-14748 when applied in accordance with WCAP-15029-A acceptable in the WCAP-15029-P-A SER. The WCAP-15029-P-A option to use a break-opening time based upon WCAP-14748, is adopted for the baffle barrel bolting.

The mechanical analysis has been performed using conservative assumptions in order to obtain results with extra margin. Some of the most significant are:

- a. When applying the hydraulic forces, no credit is taken for the stiffening effect of the fluid environment which will reduce the deflections and stresses in the structure.

01411898

01411898

- b. The multi-mass model described below is considered to have a sufficient number of degrees of freedom to represent the most important modes of vibration in the horizontal and vertical directions.

**3.6.3.3.1 Not Used**

**3.6.3.3.2 Not Used**

#### **3.6.3.3.3 Transverse and Vertical Excitation Model for Blowdown and Seismic**

The mathematical model of the RPV is a three-dimensional nonlinear finite element model which represents the dynamic characteristics of the reactor vessel and its internals in the six geometric degrees of freedom. The model consists of three concentric structural submodels connected by nonlinear impact elements and stiffness matrices, which is connected to submodel of the CRDMs and CRDM seismic platform, tie rods, and lifting legs. The first submodel represents the reactor vessel shell and associated components. The reactor vessel is restrained by six (6) reactor vessel supports (situated beneath each of four (4) nozzles and two external support pads) and by the attached primary coolant piping. Each reactor vessel support is modeled by a linear horizontal stiffness and a vertical impact element. The attached piping is represented by a stiffness matrix.

The second submodel represents the reactor core barrel (RCB), neutron panels, lower support plate, the plates, and secondary core support components. This submodel is physically located inside the first, and is connected to it by a stiffness matrix at the internals support ledge. Core barrel to vessel shell impact is represented by nonlinear elements at the core barrel flange, core barrel nozzle, and lower radial support locations.

The third and innermost submodel, represents the upper support plate, guide tubes, support columns, upper and lower core plates, and fuel. The third submodel is connected to the first and second by stiffness matrices and nonlinear elements.

Fluid-structure or hydro-elastic interaction is included in the reactor pressure vessel model for seismic evaluation. The horizontal hydro-elastic interaction is significant in the cylindrical fluid flow region between the core barrel and reactor vessel (the downcomer). Mass matrices with off-diagonal terms (horizontal degrees-of-freedom only) attach between nodes on the core barrel and reactor vessel shell.

The diagonal terms of the mass matrix are similar to the lumping of water mass to the vessel shell and core barrel. The off-diagonal terms reflect the fact that all the water mass does not participate when there is no relative motion of the vessel and core barrel. It should be pointed out that the hydrodynamic mass matrix has no artificial virtual mass effect and is derived in a straight-forward, quantitative manner.

01406407

01411898



The matrices are a function of the properties of two cylinders with a fluid in the cylindrical annulus, specifically; inside and outside radius of the annulus, density of the fluid and length of the cylinders. Vertical segmentation of the reactor core barrel allows inclusion of radii variations along the reactor core barrel height and approximates the effects of reactor core barrel deformation. These mass matrices were inserted between selected nodes on the core barrel and reactor vessel shell.

This method of modeling of the reactor internals for LOCA and seismic dynamic analyses has been approved by the USNRC (Reference 89).

The appropriate forcing functions are applied simultaneously and independently. The results from the program give the forces, displacements and deflections as functions of time for all the reactor internals components. Reactor internals response to both hot and cold leg pipe ruptures is analyzed. The forcing functions used are obtained from hydraulic analyses of the pressure and flow distribution around the entire reactor coolant system as caused by double ended severance of a reactor coolant system pipe. Since Prairie Island has received a LBB exemption for the main coolant loop piping, consideration of breaks in the main coolant loop are not required for structural evaluations. The next limiting breaks considered were the branch line breaks. The hydraulic LOCA forces for the breaks listed below are used in the reactor vessel LOCA analysis:

- Accumulator line (cold leg)
- Pressurizer surge line (hot leg)

#### **3.6.3.3.4 Vertical Excitation Model for Earthquake**

See section 3.6.3.3.3 for a description of the vertical excitation model for earthquake events.

#### **3.6.3.3.5 Transverse Excitation Model for Blowdown**

Various reactor internal components are subjected to transverse excitation during blowdown. Specifically, the barrel, guide tubes, and upper support columns are analyzed to determine their response to this excitation.

##### **Core Barrel**

For the hydraulic analysis of the pressure transients during hot leg blowdown, the maximum pressure drop across the barrel is a uniform radial compressive impulse. The barrel is then analyzed for dynamic buckling using these conditions and the following conservative assumptions: (a) The effect of the fluid environment is neglected (water stiffening is not considered); (b) the shell is treated as simply supported.

During cold leg blowdown, the upper barrel is subjected to a nonaxisymmetric expansion radial impulse which changes as the rarefaction wave propagates both around the barrel and down the outer flow annulus between vessel and barrel.

The analysis of transverse barrel response to cold leg blowdown is performed as follows:

- a. The upper core barrel is treated as a simply supported cylindrical shell of constant thickness between the upper flange weldment and the lower core barrel weldment without taking credit for the supports at the barrel midspan offered by the outlet nozzles. This assumption leads to conservative deflection estimates of the upper core barrel.
- b. The upper core barrel is analyzed as a shell with four variable sections to model the support flange, upper barrel, reduced weld section, and a portion of the lower core barrel.
- c. The barrel with the core and thermal shield, is analyzed as a beam fixed at the top and elastically supported at the lower radial support and the dynamic response is obtained.

### Guide Tubes

The dynamic loads on RCC guide tubes resulting from a loss-of-coolant accident caused by hot leg rupture or by cold leg rupture are analyzed to determine the most limiting case. The results of the analysis are reported in References 56 and 58.

The guide tubes in closest proximity to the ruptured outlet nozzle are the most severely loaded. The transverse guide tube forces during the hot leg blowdown decrease with increasing distance from the ruptured nozzle location.

A detailed structural analysis of the RCC guide tubes was performed to establish the equivalent cross section properties and elastic end support conditions. An analytical model was verified both dynamically and statically by subjecting the control rod cluster guide tube to a concentrated force applied at the transition plate. In addition, a similar tube was loaded experimentally using a triangular distribution to conservatively approximate the hydraulic loading. The experimental results consisted of a load deflection curve for the RCC guide tube plus verification of the deflection criteria to assure RCC insertion.

The response of the guide tubes to the transient loading due to blowdown may be found by utilizing the equivalent single freedom system for the guide tube using experimental results for equivalent stiffness and natural frequency.

The time dependence of the hydraulic transient loading has the form of a step function with constant slope front with a rise time to peak force of the same order of the guide tube fundamental period in water. The dynamic amplification factor in determining the response is a function of the ramp impulse rise time divided by the period of the structure.

#### Upper Support Columns

Upper support columns located close to the broken nozzle during a hot leg break will be subjected to transverse loads due to cross flow.

The loads applied to the columns were computed with a similar method to the one used for the guide tubes; i.e., taking into consideration the increase in flow across the column during the accident. The columns were studied as beams and the resulting stresses were obtained using the reduced section modulus at the body weld section.

#### **3.6.3.3.6 Transverse Excitation Model for Earthquake**

See section 3.6.3.3.3 for a description of the transverse excitation model for seismic events.

#### **3.6.3.4 Conclusions - Mechanical Analysis**

The results of the analysis, applicable to the Prairie Island design, are presented in Table 3.6-3 and Table 3.6-4. These tables summarize the maximum deflections and stresses for blowdown, seismic, and blowdown plus seismic loadings.

The stresses due to the DBE (vertical and horizontal components) were combined either by using square root sum of the squares or in a more unfavorable manner with the blowdown stresses in order to obtain the largest principal stress and deflection.

These results indicate that the maximum deflections and stress in the critical structures are below the established allowable limits. For the transverse excitation, it is shown that the upper barrel does not buckle during a hot leg break and that it has an allowable stress distribution during a cold leg break. The results for the blowdown analysis in Table 3.6-3 and Table 3.6-4 are for double ended hot and cold breaks in the main coolant piping at previous historical analytical conditions. Leak-before-break (LBB) methodology has been licensed for the main coolant piping, which precludes the need to analyze for breaks in the main coolant pipe. The next limiting breaks considered were the branch line breaks. Since the branch line breaks have break areas smaller than the double ended breaks, resulting in smaller hydraulic (mass flow and acoustic pressure) forces being applied to the reactor internals, the blowdown results in Table 3.6-3 and Table 3.6-4 bound the branch line breaks at the MUR RCS conditions.

NSAL-11-2 [Reference 92 ] addressed a non-conservative error in the lower radial support stiffness. This error potentially increases the deflections determined for MUR RCS conditions. Evaluation by Westinghouse determined that a coolable core geometry will be maintained for Prairie Island Units 1 and 2.

To assess the feasibility of crediting the RCCA insertion during a combined LOCA and seismic event, the loads on the guide tubes are calculated. The evaluation shows that the LOCA and the SSE seismic event loads were within the allowable loads that were established for 14 x 14 type guide tubes to ensure that the RCCA scram time is acceptable. A full core of 14 x 14 OFA fuel or 14 x 14 422 V + fuel, with thimble plugging devices removed for both fuel types is considered in this evaluation. Consequently, the RCCA insertion for Prairie Island Units 1 and 2 could be credited following a combined SSE and LOCA event.

### **3.7 TESTS AND INSPECTIONS**

#### **3.7.1 Reactivity Anomalies**

The incore instrumentation system is used to verify that actual power distributions in the core are satisfactory.

Nuclear flux channels are calibrated periodically when the plant is at power, using a heat balance calculation to account for discrepancies resulting from changes in the control rod pattern and core physics parameters. To eliminate possible errors in the calculations of the initial reactivity of the core and the reactivity depletion rate, the predicted relation between fuel burn-up and the boron concentration, necessary to maintain adequate control characteristics, must be adjusted (normalized) to accurately reflect actual core conditions. When full power is reached initially, and with the control rod groups in the desired positions, the boron concentration is measured and the predicted curve is adjusted to this point. As power operation proceeds, the measured boron concentration is compared with the predicted concentration and the slope of the curve relating burn-up and reactivity is compared with that predicted.

This process of normalization should be completed after about 10% of the total core burn-up. Thereafter, actual boron concentration can be compared with prediction, and the reactivity status of the core can be continuously evaluated. Any reactivity anomaly greater than 1% would be unexpected, and its occurrence would be thoroughly investigated and evaluated.

#### **3.7.2 Thermal and Hydraulic Tests and Inspections**

General hydraulic tests on models are used to confirm the design flow distributions and pressure drops (References 48, 49).

#### **3.7.3 Core Component Tests and Inspections**

To ensure conformance to all materials, components and assemblies to the design requirements, a release point program is established with the manufacturer. This requires surveillance of all raw materials, special processes, i.e., welding, heat treating, nondestructive testing, etc. and those characteristics of parts which directly affect the assembly and alignment of the reactor internals. The surveillance is accomplished by the issuance of an Inspection Release by quality control organization after conformance has been verified.

A resident quality control representative performs a surveillance/audit program at the manufacturer's facility and witnesses the required tests and inspections and issues the inspection releases. An example is the radiographic examination of the welds joining core barrel shell courses.

Components and materials supplied to the assembly manufacturer are subjected to a similar program. Quality Control engineers develop inspection plans for all raw materials, components and assemblies. Each level of manufacturing is evaluated by a qualified inspector for conformance, i.e. witnessing the ultrasonic testing of core plant raw material. Upon completion of specified events, all documentation is audited prior to releasing the material or component for further manufacturing. All documentation and inspection releases are maintained in the quality control central records section. All materials are traceable to the mill heat number.

In conclusion a set of "as built" dimensions are taken to verify conformance to the design requirements and assure proper fitup between the reactor internals and the reactor pressure vessel.

### **3.7.3.1 Fuel Quality Control**

Quality Control philosophy is generally based on the following inspections being performed to a 95% confidence that at least 95% of the product meets specification, unless otherwise noted, using either a hypergeometric function with zero defectives for small lots or the latest revision of Mil-105D for large lots. The following describes the fuel manufacturing operation and inspection.

- a. Component Parts - All parts received are inspected to a 95/95 confidence level. The characteristics inspected depends upon the component parts and includes dimensional, visual, check audits of test reports, material certification and non-destructive testing such as X-ray and ultrasonic. Applicable quality plans specify all attributes for test and inspection, their classification, and the sampling frequency for each attribute for each purchase.
- b. Nuclear Materials - Enriched uranium hexafluoride ( $\text{UF}_6$ ) is received from various gaseous diffusion plants. An independent sample is analyzed for total U and U-235 content. The cylinders are check weighed upon receipt to confirm the gross weight. The  $\text{UF}_6$  is vaporized, hydrolized with water, treated with ammonia to precipitate ammonium diuranate which is subsequently calcined to produce uranium dioxide ( $\text{UO}_2$ ) powder. The  $\text{UO}_2$  powder is then pressed into pellets, sintered, and ground to required dimensions.

Inspection is performed to a 95/95 level for the dimensional characteristics such as diameter, length and squareness of ends. Additional visual inspections are performed for cracks, chips and porosity, according to standards established at the beginning of production. Density is determined in terms of weight per unit length and is plotted on zone charts used in controlling the process. Chemical analyses are taken on a sample basis throughout pellet production.

- c. Fuel Rods - Pellets are outgassed at high temperatures in a vacuum oven, placed in a trough to a pre-established length, weighed and loaded into accepted cladding tubing which has previously had a bottom end cap welded and serialized. After the rods are loaded and pressurized, the final end cap is welded on. All fabricated rods are leak tested, ultrasonically tested or X-rayed and dimensionally inspected.
- d. Fuel Assemblies - Acceptable rods are assembled into five bundles in accordance with a predetermined matrix for the individual bundle. After final dimensional bundle inspection and verification, the fuel bundles are sent to storage for subsequent shipment to the plant.
- e. Other Inspection - The following inspection will be performed as part of routine inspection operation:
  - 1. Measurements other than those specified above which are critical to thermal and hydraulic analyses are obtained to enable evaluation of manufacturing variations to predetermined specifications.
  - 2. Tool and gage inspection and control including standardization to primary and secondary working standards. Tool inspection is performed at prescribed intervals on all serialized tools. Complete records are kept of calibration and condition of tools.
  - 3. Check audit inspection of all inspection activities and records to assure that prescribed methods are followed and that all records are correct and properly maintained.
  - 4. Surveillance of outside contractors, including approval of standards and methods are performed where necessary. However, all final acceptance is based upon receipt inspection.

To prevent the possibility of mixing enrichments during fuel manufacture and assembly, meticulous process control is exercised.

The  $\text{UO}_2$  powder is in sealed containers, the contents of which are fully identified both by descriptive tagging and preselected color coding.

Powder withdrawal from storage can be made by one authorized group only who direct the powder to the correct pellet production line. All pellet production lines are physically separated from each other and pellets of only a single enrichment and density are produced in a given production line.

01271335

01284359

Finished pellets are placed on trays having the same descriptive tagging as the powder containers and transferred to segregated storage racks. Physical barriers prevent mixing of pellets of different densities and enrichments in this storage area. Unused powder and substandard pellets to be reprocessed are returned to storage in coded containers.

Loading of the pellets into the cladding is again accomplished in isolated production lines.

At the time of loading, the fuel tube end plug identification number is checked with the enrichment identification of the pellet storage tray.

After the fuel rods are installed, an inspector verifies that all fuel rods in an assembly have the correct end plug identification, and that the top nozzle to be used on the assembly carries the correct identification character. The top nozzle identification then becomes the permanent description of the fuel contained in the assembly.



### **3.8 REFERENCES**

1. "Power Distribution Control in Westinghouse Pressurized Water Reactors," WCAP-7811, December 1971.
2. Deleted
3. Deleted
4. Deleted
5. XN-NF-78-34(P), Exxon Nuclear Company, "Generic Mechanical and Thermal Hydraulic Design for Exxon Nuclear 14x14 Reload Fuel Assemblies with Zircaloy Guide Tubes for Westinghouse 2-Loop Pressurized Water Reactors," November 1978.
6. Deleted
7. Deleted
8. Deleted
9. Deleted
10. Deleted
11. Deleted
12. Deleted
13. Deleted
14. Deleted
15. Deleted
16. Deleted
17. Deleted
18. Deleted
19. Deleted
20. Deleted
21. Deleted
22. Deleted
23. Deleted
24. Deleted
25. H.W. Wilson, K.K. Yoon, and D.L. Baty, "The Effect of Fuel Rod Design on SCC Susceptibility", "ANS Light Water Reactor Fuel Performance Conferences," Portland, OR. April 29-May 3, 1979.
26. A.A. Bauer, L.M. Lowry, W.J. Gallagher, and A.J. Markworth, "Evaluating Strength and Ductility of Irradiated Zircaloy -Quarterly Progress Report July through September 1977," BMI-NUREG-1985, October 1977.
27. R.A. Lorenz, J.L. Collings, S.R. Manning, "Fission Product Release From Simulated LWR Fuel," NUREG/CR-0274, ORNL/NUREG/TM-154, October 1978.

28. M. Peels, H. Stehle, and E. Steinberg, "Out-of-Pile Testing of Iodine Stress Corrosion Cracking in Zircaloy Tubing in Relation to the PCI-Phenomenon", Fourth International Conference on Zirconium in the Nuclear Industry, 1978.
29. Nukleare Sicherheit, "Halbjahresbericht 1977/1", KFK 2500, Kernforschungszentrum, Karlsruhe, December 1977.
30. A.K. Miller, K.D. Challenger, E. Smith, G.V. Ranjan, and R.C. Cipolla, "Zircaloy Cladding Deformation and Fracture Analysis", EPRI NP-856, August 1978.
31. L.F. VanSwam, D.B. Knorr, R.M. Pelloux, and J.F. Shewbridge, "Relationship Between Contractile Strain Ratio R and Texture in Zirconium Alloy Tubing", Metallurgical Transactions Vol. 10A, April 1979.
32. A.A. Bauer, L.M. Lowry, and J.S. Perrin, "Progress on Evaluating Strength and Ductility of Irradiated Zircaloy During July through September 1974", BMI-1938, September 1975.
33. A.A. Bauer, L.M. Lowry, and J.S. Perrin, "Evaluating Strength and Ductility of Irradiated Zircaloy - Quarterly Progress Report for October through December 1975", BMI-1942, December 1975.
34. A.A. Bauer, L.M. Lowry, and J.S. Perrin, "Evaluating Strength and Ductility of Irradiated Zircaloy - Quarterly Progress Report January through March 1976", BMI-NUREG-1928, March 1976.
35. A.A. Bauer, L.M. Lowry, and J.S. Perrin, "Evaluating Strength and Ductility of Irradiated Zircaloy - Quarterly Progress Report April through June 1976", BMI-NUREG-1956, July 1976.
36. A.A. Bauer, L.M. Lowry, and J.S. Perrin, "Evaluating Strength and Ductility of Irradiated Zircaloy - Quarterly Progress Report July through September 1976", BMI-NUREG-1961, October 1976.
37. A.A. Bauer, L.M. Lowry, and J.S. Perrin, "Evaluating Strength and Ductility of Irradiated Zircaloy - Quarterly Progress Report October through December 1976", BMI-NUREG-1967, January 1977.
38. A.A. Bauer, L.M. Lowry, and J.S. Perrin, "Evaluating Strength and Ductility of Irradiated Zircaloy - Quarterly Progress Report January through March 1977", BMI-NUREG-1971, April 1977.
39. A.A. Bauer, L.M. Lowry, and J.S. Perrin, "Evaluating Strength and Ductility of Irradiated Zircaloy - Quarterly Progress Report April through June 1977", BMI-NUREG-1976, July 1977.

- 
40. A.A. Bauer, L.M. Lowry, W.J. Gallagher, and A.J. Markworth, "Evaluating Strength and Ductility of Irradiated Zircaloy - Quarterly Progress Report October through December 1977", NUREG/CR-0026, BMI-1992, January 1978.
  41. A.A. Bauer, L.M. Lowry, W.J. Gallagher, and A.J. Markworth, "Evaluating Strength and Ductility of Irradiated Zircaloy - Quarterly Progress Report January through March 1978", NUREG/CR-0085, BMI-2000, June 1978.
  42. W.J. O'Donnel and B.F. Langer, "Fatigue Design Bases for Zircaloy Components", "Nuclear Science and Engineering, Volume 20, January 1964.
  43. J.J. Holmes, J.A. Williams, D.H. Nyman, J.C. Tobin, "In-Reactor Creep of Cold-Worked Zircaloy-2", "Flow and Fracture of Metals and Alloys in Nuclear Environments", ASTM, STP-380, 1964.
  44. G.J. Bohm, Indian Point Unit No. 2 "Reactor Internals Mechanical Analysis for Blowdown Excitation," WCAP-7822, December 1971. (1709/1827)
  45. Deleted
  46. Deleted
  47. Deleted
  48. G. Hetsroni, "Hydraulic Tests of the San Onofre Reactor Model", WCAP-3269-8 (1964).
  49. G. Hetsroni, "Studies of the Connecticut-Yankee Hydraulic Model," WCAP-2761 (1965).
  50. Deleted
  51. Deleted
  52. Deleted
  53. Deleted
  54. Letter, D. M. Musolf (NSP) to the Director of NRR (NRC), "Safety Evaluation for RCC Guide Thimble Plug Removal", April 22, 1985. (19913/1217)
  55. Letter, E. J. Butcher (NRC) to D. M. Musolf (NSP), "Rod Cluster Control Guide Thimble Plug Removal (SER)", October 18, 1985. (19914/1039)
  56. J.T. Land, "Northern States Power Upper Internals Replacement Design Report, Unit 1", WNEP-8570, December 20, 1985. (2186/0877)

57. J.T. Land, "Northern States Power Thermocouple Column Assembly Replacement Design Report, Unit 1", WNEP-8571, December 16, 1985. (2186/0735)
58. J.T. Land, "Northern States Power Upper Internals Replacement Design Report, Unit 2", WNEP-8628, May 12, 1986. (2186/0954)
59. J.T. Land, "Northern States Power Thermocouple Column Assembly Replacement Design Report, Unit 2", WNEP-8627, May 12, 1986. (2186/0792)
60. WCAP-11066 "Prairie Island Unit 1 Reactor Vessel Upper Internals Replacement Safety Evaluation", February 12, 1986.
61. WCAP-8691, Revision 1, "Fuel Rod Bow Evaluation," July, 1979.
62. Deleted
63. Deleted
64. WCAP 7308-L-P-A Rev. 1 "Evaluation of Nuclear Hot Channel Uncertainties," June 1988.
65. WCAP-12610-P-A, "VANTAGE + Fuel Assembly Reference Core Report," April 1995.
66. W.H. Slagle, "Compatibility Assessment for the Westinghouse 14x14 VANTAGE+ Fuel Assemblies in Prairie Island Units 1 & 2," August 1993.
67. D.H. Risher, "Safety Analysis for the Revised Fuel Rod Internal Pressure Design Basis," WCAP-8963-A, August 1978.
68. "Request for Reduction in Fuel Assembly Burnup Limit for Calculation of Maximum Rod Bow Penalty," letter, C. Berlinger (NRC) to E. P. Rabe, Jr. (Westinghouse), June 18, 1986.
69. WCAP - 10216 - P-A, Revision 1A, "Relaxation of Constant Axial Offset Control/ F<sub>q</sub> Surveillance Technical Specification."

70. Deleted
71. WCAP-13360-P-A, "Westinghouse Dynamic Rod Worth Measurement Technique"
72. Safety Evaluation by the Office of Nuclear Reactor Regulation Relating to Topical WCAP-13360 Westinghouse Dynamic Rod Worth Measurement Technique TAC No. M83235, January 5, 1996.
73. L. S. Tong, "Prediction of Departure from Nucleate Boiling for an Axially Non-Uniform Heat Flux Distribution," Journal of Nuclear Energy, Vol. 21, pp. 241-248 (1967).
74. WCAP-8762-P-A, "New Westinghouse Correlation WRB-1 for Predicting Critical Heat Flux in Rod Bundles with Mixing Vane Grids," dated September 1978 (approved July 1984).
75. Letter from C. O. Thomas (NRC) to E. P. Rahe (Westinghouse), "SER on the Applicability of WRB-1 to Westinghouse 14x14 and 15x15 OFA," June 29, 1984.
76. J. Weisman, A. H. Wenzel, L. S. Tong, D. Fitzsimmons, W., Thorne and J. Batch, "Experimental Determination of the Departure from Nucleate Boiling in Large Rod Bundles at High Pressure," AIChE, Preprint 29, 9th National Heat Transfer Conference, 1967, Seattle, Washington.
77. S. Tong, H. Chelemer, J. E. Casterline and B. Matzner, "Critical Heat Flux (DNB) in Square and Triangular Array Rod Bundles," JSME, Semi-International Symposium, Paper #256, 1967, Tokyo, Japan.
78. Boure, J. A., Bergles, A. E., and Tong, L. S., "Review of Two-Phase Flow Instability," Nucl. Engr. Design 25 (1973) p. 165-192.
79. Lahey, R. T., and Moody, F. J., "The Thermal Hydraulics of a Boiling Water Reactor," American Nuclear Society, 1977.
80. Saha, P., Ishii, M., and Zuber, N., "An Experimental Investigation of the Thermally Induced Flow Oscillations in Two-Phase Systems," J. of Heat Transfer, November 1976, pp. 616-622.
81. Summer, Virgil C., FSAR, Docket #50-395.
82. Byron/Braidwood FSAR, Docket #50-456.

83. Comanche Peak FSAR, Docket #50-445.
84. Kakac, S., Veziroglu, T. N., Akyuzlu, K., Berkol, O., "Stained and Transient Boiling Flow Instabilities in a Cross-Connected Four-Parallel-Channel Upflow System," Proc. of 5th International Heat Transfer Conference, Tokyo, September 3-7, 1974.
85. Kao, H. S., Morgan, C. D., and Parker, W. B., "Prediction of Flow Oscillation in Reactor Core Channel," Trans. ANS, Vol. 16, 1973, pp. 212-213.
86. Friedland, A. J., Ray, S., "Revised Thermal Design Procedure," WCAP-11397-P-A (Proprietary), WCAP-11397-A (Nonproprietary), dated April 1989.
87. Foster, J. P., Sidener, S. "Westinghouse Improved Performance Analysis and Design Model (PAD 4.0)," WCAP-15063-P-A, Revision 1, with Errata, July 2000.
88. Slagle, W. H., "Revisions to Design Criteria," WCAP-10125-P-A, Addendum 1-A, May 2003.
89. Poploski, M., Leidich, A., "Prairie Island Units 1&2 422V + Reload Transition Safety Report", dated May 2008.
90. WCAP-9401-PA, "Verification Testing and Analysis of the 17 x 17 Optimized Fuel Assembly – Approved Version, "Westinghouse August 1981.
91. Shah, H. H., "Optimized ZIRLO," WCAP-12610-P-A & CENPD-404-P-A Addendum 1-A, July 2006.
92. Westinghouse Nuclear Safety Advisory Letter, NSAL-11-2, "Impact of Change in Lower Radial Key Stiffness Value", June 28, 2011.
93. Letter, L-PI-08-047, PINGP to USNRC, "License Amendment Request for Technical Specification Changes to Allow Use of Westinghouse 0.422-inch OD 14x14 VANTAGE+ Fuel", dated June 26, 2008.
94. WCAP-9735 Rev. 2 (Proprietary), WCAP-9736 Rev. 1 (Non-Proprietary), "MULTIFLEX 3.0, A FORTRAN-IV Computer Program for Analyzing Thermal-Hydraulic-Structural System Dynamics Advances Beam Model," Takeuchi, K. et al, February, 1998.
95. WCAP-15029-P-A, Revision 1, "Westinghouse Methodology for Evaluating the Acceptability of Baffle-Former-Barrel Bolting Distribution Under Faulted Load Conditions", January 1999.
96. Garde, A., et. al., "Westinghouse Clad Corrosion Model for ZIRLO and Optimized ZIRLO," WCAP-12610-P-A & CENPD-404-P-A Addendum 2-A, October 2013.

**TABLE 3.1-1 FUEL ANALYSIS DESIGNS**

	<b>Westinghouse 422 Vantage +</b>	<b>Westinghouse 400 Vantage+</b>
Rod Pitch, in	0.556	0.556
Active Fuel Length (in)	143.25	144
Fuel Pellet OD, in	0.3659	0.3444
Clad OD, in	0.422	0.4000
Clad ID, in	0.3734	0.3514
Clad Thickness, in	0.0243	0.0243
Diametral Gap, in	0.0075	0.0070
Cell Water-To-Fuel Volume Ratio	1.61	1.97
Pellet Density (%TD)	95	95
Dishing Volume (%)	1.19	1.19
Assembly Weight, KgU	393*	351*
Active Surface Area/Assembly (ft <sup>2</sup> )	236.1	225.0
Flow Area/Assembly (in <sup>2</sup> )	32.234	34.79
Average Heat Flux (MBtu/hr-ft <sup>2</sup> )	0.2007	0.2107**
Average Linear Power (kw/ft)	6.50	6.47**
Fuel Rods/Assembly	179	179
Guide Tubes/Assembly	16	16
Instrument Tubes/Assembly**	1	1
Cladding Material	ZIRLO/Optimized ZIRLO	ZIRLO
Number of Grids/Assembly	7	7
Grid Material		
Middle 5 grids	ZIRLO	Zr-4
2 end grids	Inc.718	Inc.718

01284359

01284359

\* Non-poisoned

\*\* Based on 1677MWt.

TABLE 3.2-1 THERMAL AND HYDRAULIC DESIGN PARAMETERS

Parameter	Value	
Reactor Power, MWt <sup>(4)</sup>	1683	
NSSS Power, MWt <sup>(4)</sup>	1690	
Heat generated in fuel, %	97.4	
Maximum Thermal Overpower, %	118	
Nominal System Pressure, psia	2250	
Hot Channel Factors		
Heat Flux - Nuclear, $F_Q^N$	2.50	
Enthalpy rise - Nuclear, $F_{\Delta H}^N$	1.77	
Reactor Coolant Flow		
Total Minimum Core Flow Rate, gpm	167,320	
RCS Minimum Flow Rate, gpm/loop	89,000	
Core Bypass Flow, %	6.0	
Reactor Coolant Temperature <sup>(1) (3)</sup>		
Vessel/Core Inlet, deg-F	527.4	
Vessel Average, deg-F	560.0	
Core Average, deg-F	563.3	
Core Outlet, deg-F	596.4	
Vessel Outlet, deg-F	592.6	
Core Heat Transfer <sup>(1)</sup>	<u>400 V +</u>	<u>422 V +</u>
Active Heat Transfer Surface Area, ft <sup>2</sup>	27,020	28,507
Average Heat Flux, Btu/hr-ft <sup>2</sup>	211,767	200,722
DNB Ratio		
Minimum DNB Ration at Nominal Power Conditions	2.08	2.35
Pressure Drop <sup>(2)</sup>		
Across Core at 98,500 gpm/loop, psi	26.08	25.24
Across Assembly at 98,500 gpm/loop, psi	20.07	19.48

01193868  
0118331601193868  
01183316

<sup>1</sup> Based on 1677 MWt core power, 178,000 gpm flow rate, 6.0% bypass flow, 2250 psia system pressure, 560 degree Tave.

<sup>2</sup> Pressure drop is based on 201,400 gpm best estimate calculated flow, 4% bypass flow, 1683 MWt core power.

<sup>3</sup> These temperatures were calculated at nominal 1677 MWt. conditions.

<sup>4</sup> Current enveloping design power limit.



TABLE 3.6-1 REACTOR INTERNALS ALLOWABLE STRESS CRITERIA

Method of Analysis		Load, or Stress [Note (6)]	Design Limits	
System F-1322.1	Component F-1322.2		Components [Notes (3), (6)]	Component Supports [Note (3)]
Elastic	Elastic	Stress NB-3221, NB-3230 F-1323.1	$\left. \begin{matrix} 2.4S_m \\ 0.7S_u \\ 0.7S_y \end{matrix} \right\}^{**}$ for materials Table I - 1.2 for materials Table I - 1.1 [Note (1)] Alternative Limits : Valves (F - 1350), in preparation Piping (F - 1360), pressure $\leq 2 \times$ Design Pressure $\left. \begin{matrix} 3.0S_m \\ \text{[Eq. (9), NB-3652]} \end{matrix} \right\}$	$\left. \begin{matrix} 1.5S_m \\ 1.2S_y \end{matrix} \right\}^*$ but not $> 0.7S_u$ [Note(1)]
	Collapse load NB-3213.22	Load P F-1323.2 [Note (7)]	$0.9P_c$ based on $S_y = 2.3S_m$ or on $P_c$ derived from F-1321.1(d) or F-1321.3(a) [Notes (2), (7)]	$\left. \begin{matrix} 1.5S_m \\ 1.2S_y \end{matrix} \right\}^*$ but not $> 0.7S_u$ [Note(1)]
	Stress ratio F-1321.2(a)	Load $P_l$ , Stress $S_{ap}$ F-1321.2(c) F-1323.3	$\left. \begin{matrix} 3.0S_m \\ 0.7S_u \end{matrix} \right\}^{**}$ for loads $P_r$ [Note (4)]	Same as components
Inelastic	Elastic	Stress F-1324.1	$\left. \begin{matrix} 0.7S_u \\ S_y + (S_u - S_y) / 3 \end{matrix} \right\}^*$ [Note(1)]	$\left. \begin{matrix} 0.7S_u \\ S_y + (S_u - S_y) / 3 \end{matrix} \right\}^*$ [Note(1)]
	Collapse load	Load P F-1324.2	$0.9P_c$ based on $S_y = 2.3S_m$ or on $P_c$ derived from F-1321.1(d) or F-1321.3(a)	$\left. \begin{matrix} 1.5S_m \\ 1.2S_y \end{matrix} \right\}^*$ but not $> 0.7S_u$
	Stress ratio	Load $P_r$ , Stress $S_{ap}$ F-1324.3	$\left. \begin{matrix} 3.0S_m \\ 0.7S_u \end{matrix} \right\}^{**}$ for loads $P_r$ [Note (4)]	Same as components
	Plastic instability F-1321.1(e)	Load P F-1324.4	$0.7P_l$ or loads $P \leq P_m$ , where $P_m = S_y + (S_l - S_y) / 3$ [Note (5)]	Same as components
	Strain limit load	Load P F-1321.1(f) F-1324.5	$0.7P_l$ or loads $P \leq P_m$ , where $P_m = S_y + (S_l - S_y) / 3$ but not $> P_s$ [Note (8)]	Same as components
	Inelastic	Stress F-1324.6	$\left. \begin{matrix} 0.7S_u \\ S_y + (S_u - S_y) / 3 \end{matrix} \right\}^*$ [Note (1)]	Same as components

\* Use greater of limits specified.

\*\* Use lesser of limits specified.

NOTES:

- (1)  $S_u$  value at temperature shall be specified and justified in Design Report.
- (2)  $P_c$  denotes the collapse load based on lower bound theorem of limit analyses or as defined in F-1321.1(d).
- (3) The Design Limits selected from this Table shall be used in conjunction with F-1323 and F-1324, as applicable, in order to determine the limits for  $P_m$ ,  $P_l$ , and  $P_b$ .
- (4) Higher limits for  $S_{ap}$  may be used as specified in A-9000, where the type of stress field is taken into account.
- (5)  $S_l$  is the true effective stress associated with plastic instability (F-1324.4).
- (6) For compressive loads or stresses, the stability requirements of F-1325 shall be met.
- (7) This method is not permitted if deformation limits are stated in Design Specifications.
- (8)  $P_s$  denotes the load associated with the strain limit placed on the component [F-1321.1(f)].

01359843

---

**TABLE 3.6-2**

**DELETED**

01186822

# PRAIRIE ISLAND UPDATED SAFETY ANALYSIS REPORT

USAR Section 3

Revision 23

**TABLE 3.6-3 MAXIMUM DEFLECTIONS UNDER BLOWDOWN (INCHES)  
(1-MILLESECOND DOUBLE-ENDED BREAK)**

Component	Cold Leg	Hot Leg	Seismic Horizontal	Maximum Total	Allowable	No Loss of Function
<b>Upper barrel</b>						
- radial inward	0.0	0.064	0.002	0.066	2.0	4.0
- radial outward	0.093	0.021	0.002	0.095	0.5	1.0
Upper core plate	0.045	NL*	0	0.045	0.100 <sup>3</sup>	0.150
RCC Guide (26)		***	NL (All)	***	1.0 (26)	1.15 (26)
Tubes (deflection as a beam) (3)		**	NL (All)	**	1.0 (26)	1.15 (26)
Total (29)						
Fuel Assembly Thimbles (cross section distortion)	0	0	0	0	0.036	0.072

\* Not Limiting

\*\* Greater than No Loss of Function

\*\*\* Less than Allowable

01-006

01-006

<sup>3</sup> Only to assure that the plate will not touch a guide tube.

# PRAIRIE ISLAND UPDATED SAFETY ANALYSIS REPORT

USAR Section 3

Revision 31

**TABLE 3.6-4 SUMMARY OF MAXIMUM STRESS INTENSITIES (PSI)  
(1-MILLISECOND PIPE BREAK AND SEISMICS)**

Component	Hot Leg Break		Cold Leg Break		Maximum Total Seismic		Maximum Total Blowdown Plus Seismic
	Maximum Membrane	Maximum Total	Maximum Membrane	Maximum Total	Vertical	Horizontal	
Barrel (Girth weld)	NL **	NL	26,050	45,300	8,400	1,882	34,450 ***
Barrel - Flange (weld)	NL	NL	NL	NL	NL	NL	NL
Fuel Assembly Top Nozzle Plate	-	10,380	0	850	0	0	10,380
Fuel Assembly Bottom Nozzle Plate	0	44,060	0	25,080	0	0	44,060
Upper Support Columns	1,771	29,366	13,663	18,098	---	---	31,789 ***
Allowable Stress, Sm: Sm At 588°F = 16,600 psi *							
maximum membrane stress = $P_m$ = 2.4 Sm = 39,800 psi							
maximum total stress = $P_m + P_b$ = 49,800 psi							

\* Per winter 1969 Addenda ASME Section III Code

\*\* Not Limiting

\*\*\* SRRS (Square root sum of square of DBE + LOCA, Cold Leg Break Limiting)

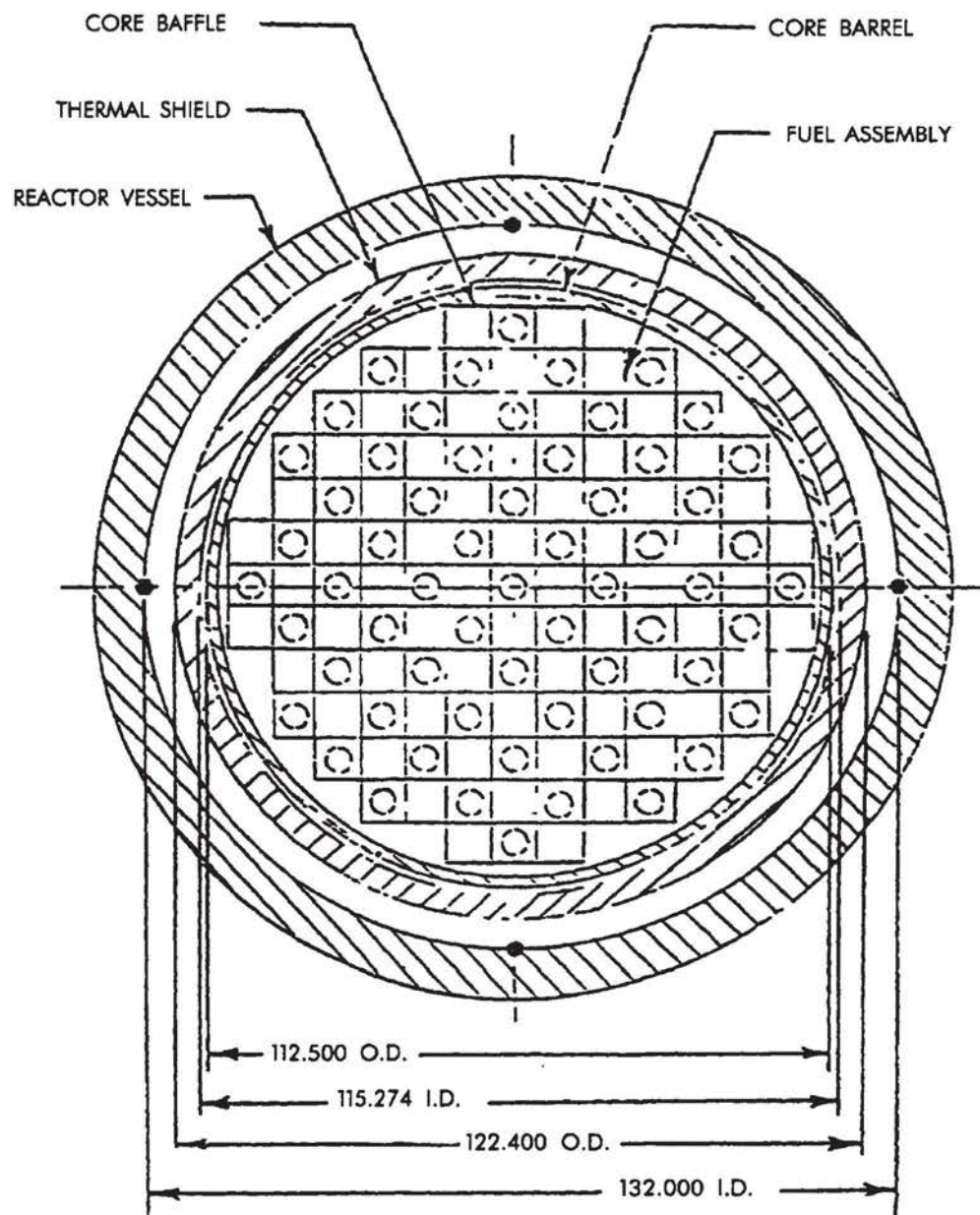
01193868

# ***PRAIRIE ISLAND UPDATED SAFETY ANALYSIS REPORT***

USAR  
Revision 0  
Page ?-1

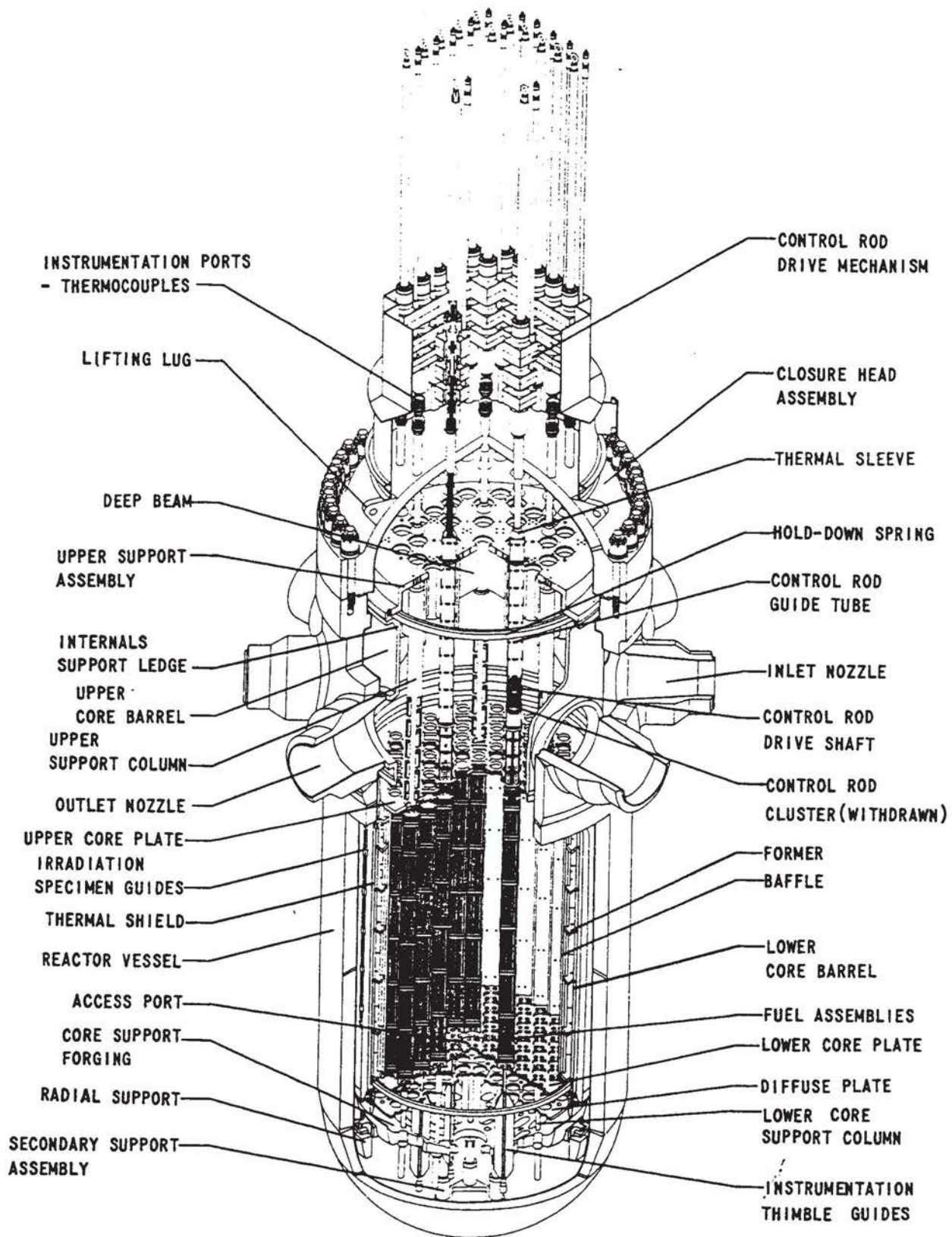
---

XXXXXXXXXXXX



REACTOR CORE CROSS SECTION

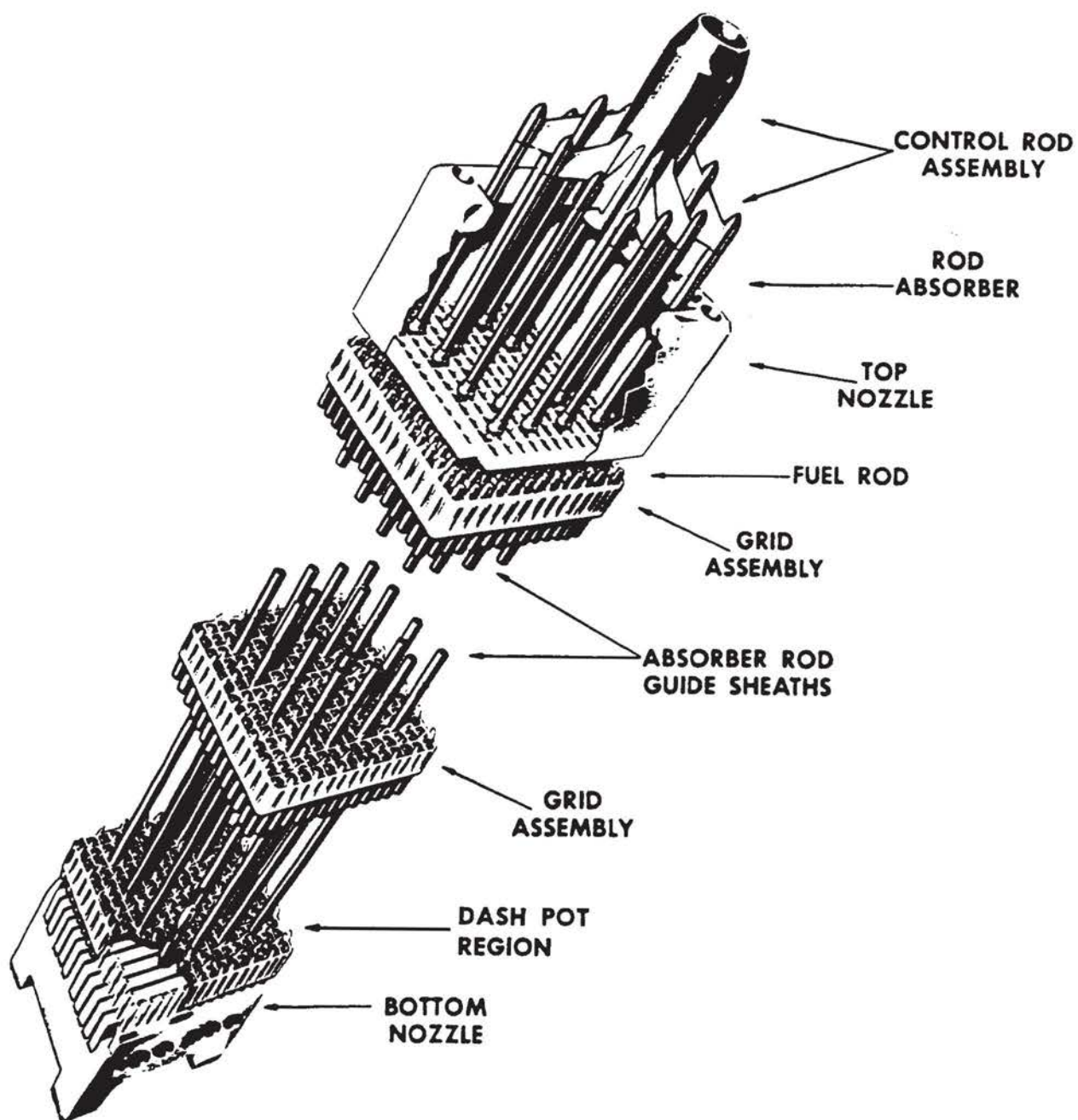
DWN	T. MILLER	DATE	6-23-99	NORTHERN STATES POWER COMPANY	SCALE	NONE
CHECKED		CAD FILE	U03101.DGN	PRAIRIE ISLAND NUCLEAR GENERATING PLANT	<b>FIGURE 3.1-1 REV. 23</b>	
				RED WING MINNESOTA		



TYPICAL REACTOR VESSEL AND INTERNALS

OWN T. MILLER	DATE 6-23-99	NORTHERN STATES POWER COMPANY PRAIRIE ISLAND NUCLEAR GENERATING PLANT RED WING MINNESOTA	SCALE: NONE	FIGURE 3.1-2 REV. 18
CHECKED	CAD FILE U03102.DGN			

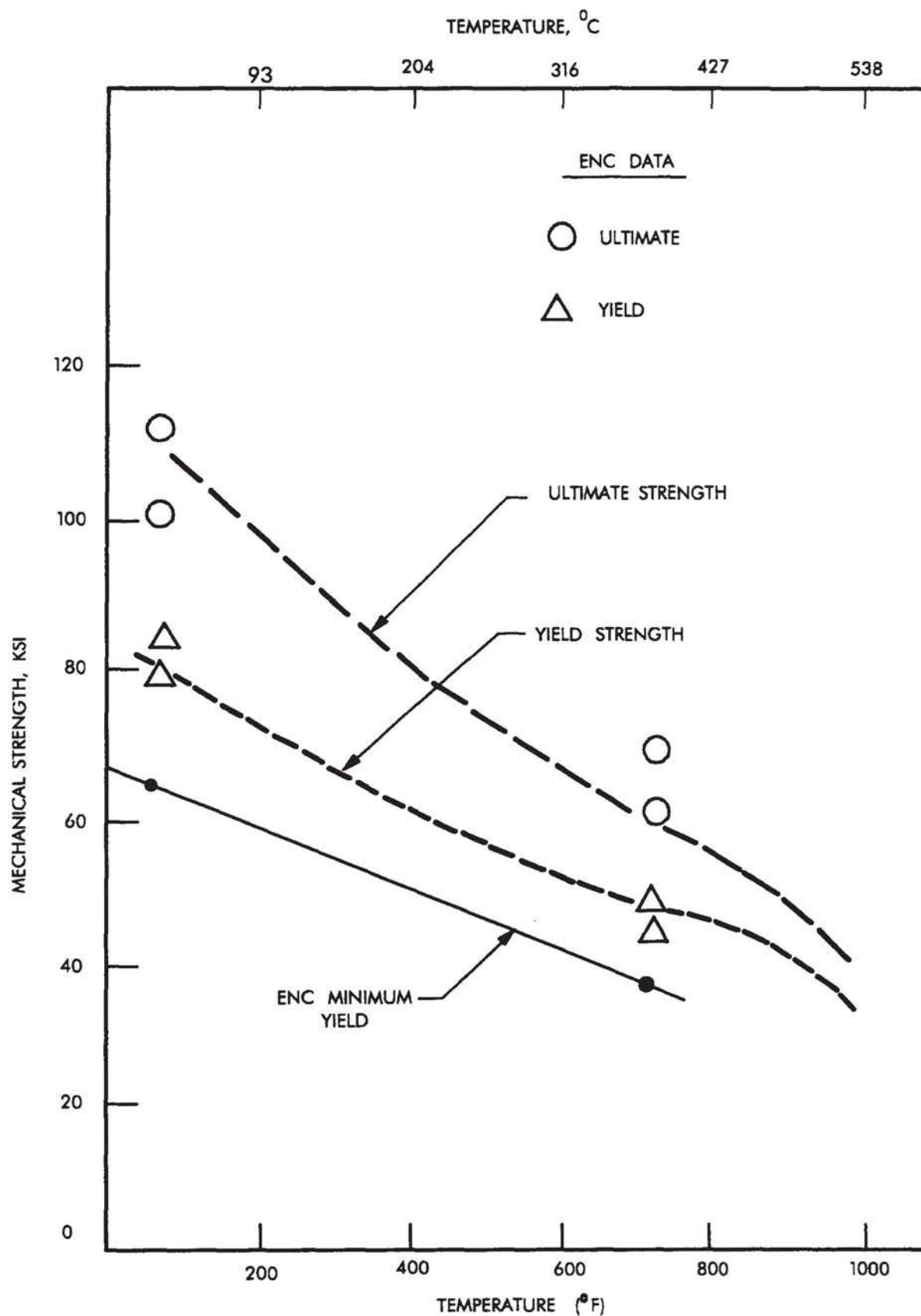




TYPICAL ROD CLUSTER CONTROL ASSEMBLY

OWN	T. MILLER	DATE	6-23-89	NORTHERN STATES POWER COMPANY	SCALE: NONE
CHECKED		CAD		PRAIRIE ISLAND NUCLEAR GENERATING PLANT	FIGURE 3.1-3 REV. 18
		FILE	U03103.DGN	RED WING MINNESOTA	



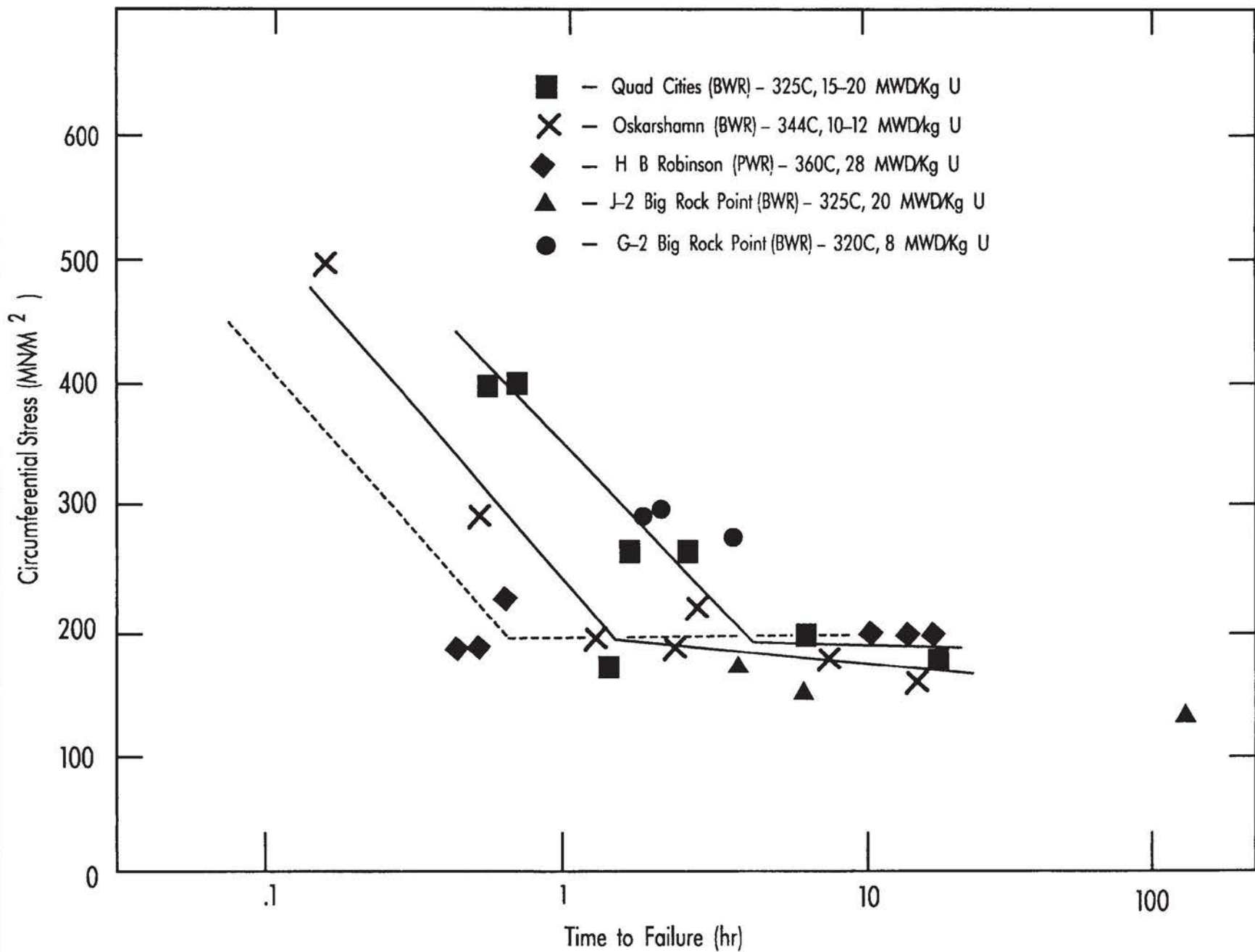


MECHANICAL STRENGTH OF ENC ZIRCALOY-4  
TUBING VERSUS TEMPERATURE

DWN T. MILLER	DATE 6-23-99	NORTHERN STATES POWER COMPANY PRAIRIE ISLAND NUCLEAR GENERATING PLANT RED WING MINNESOTA	SCALE: NONE	
CHECKED	CAD FILE U03401.DGN		FIGURE 3.4-1 REV. 23	

DWN T. MILLER	DATE 6-23-99	NORTHERN STATES POWER COMPANY PRAIRIE ISLAND NUCLEAR GENERATING PLANT RED WING, MINNESOTA	SCALE : NONE
CHECKED	CAD FILE U03402.DGN		FIGURE 3.4-2 REV. 18

# MECHANICAL STRESS THRESHOLD FOR IRRADIATED ZIRCALOY CLADDING TESTED IN AN IODINE ENVIRONMENT

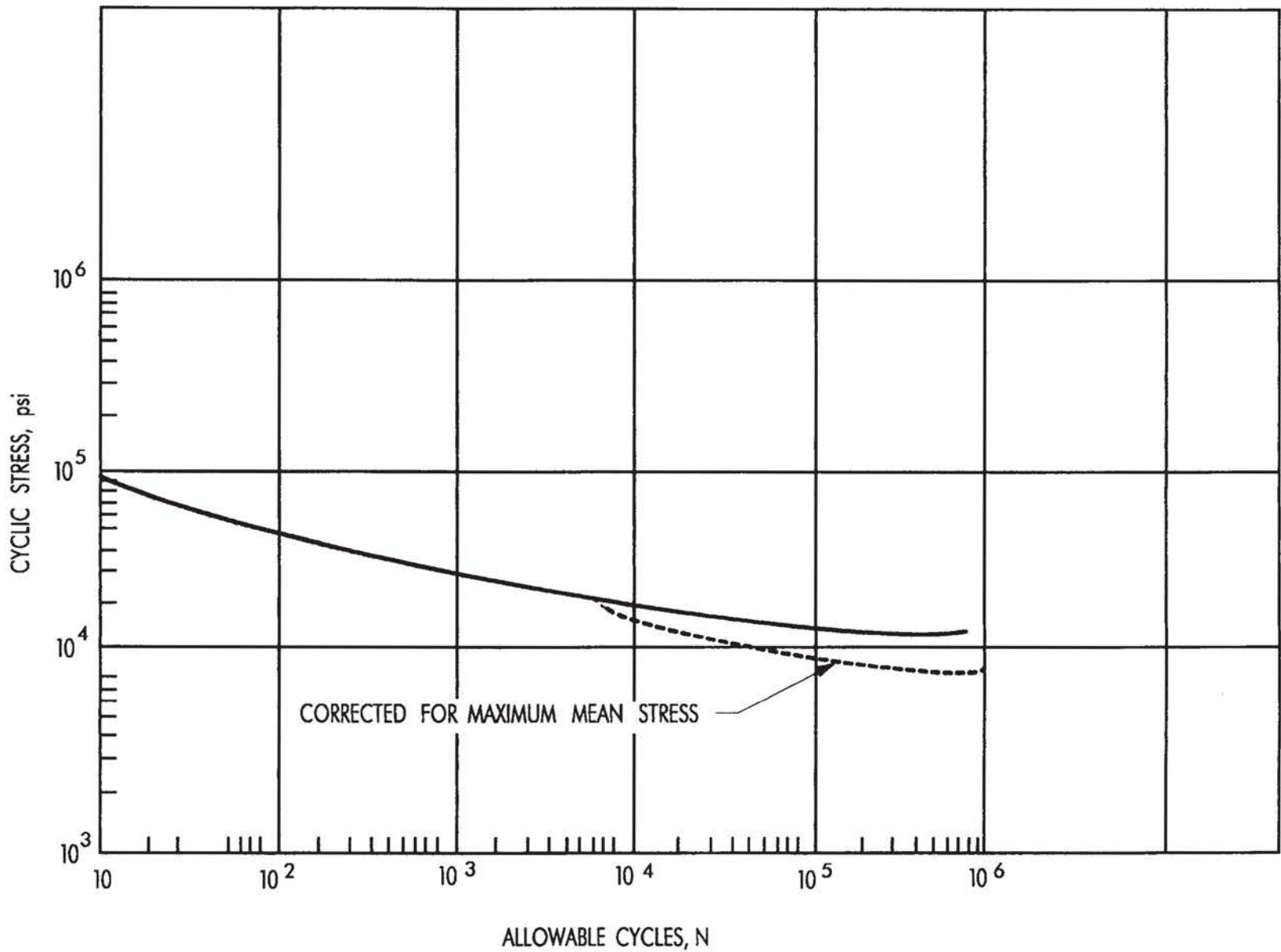


DWN	T. MILLER	DATE	6-23-99
CHECKED		CAD FILE	U03403.DGN

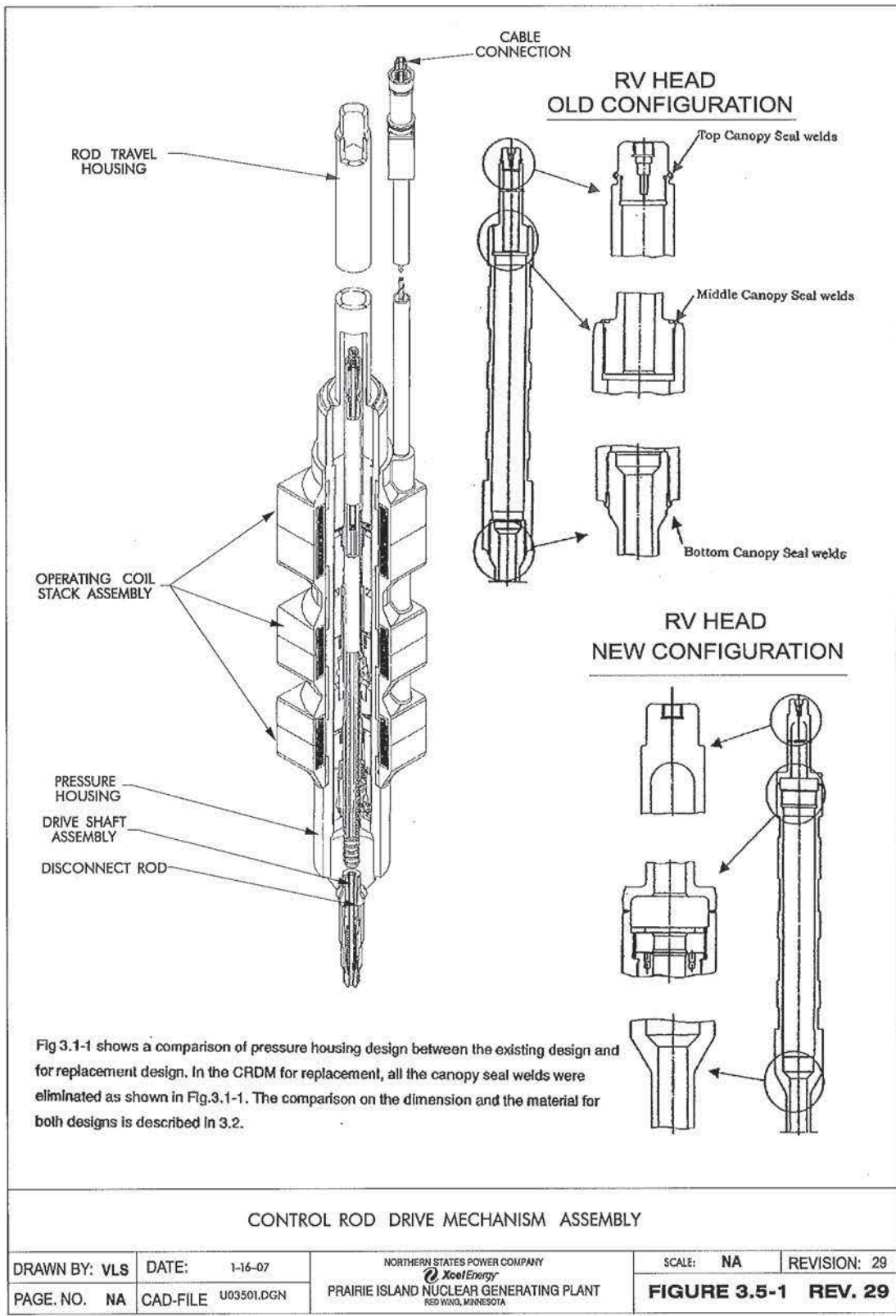
NORTHERN STATES POWER COMPANY	
PRAIRIE ISLAND NUCLEAR GENERATING PLANT	
RED WING, MINNESOTA	

SCALE : NONE	FIGURE 3.4-3	REV. 18
--------------	--------------	---------

# CYCLIC FATIGUE DESIGN CURVE

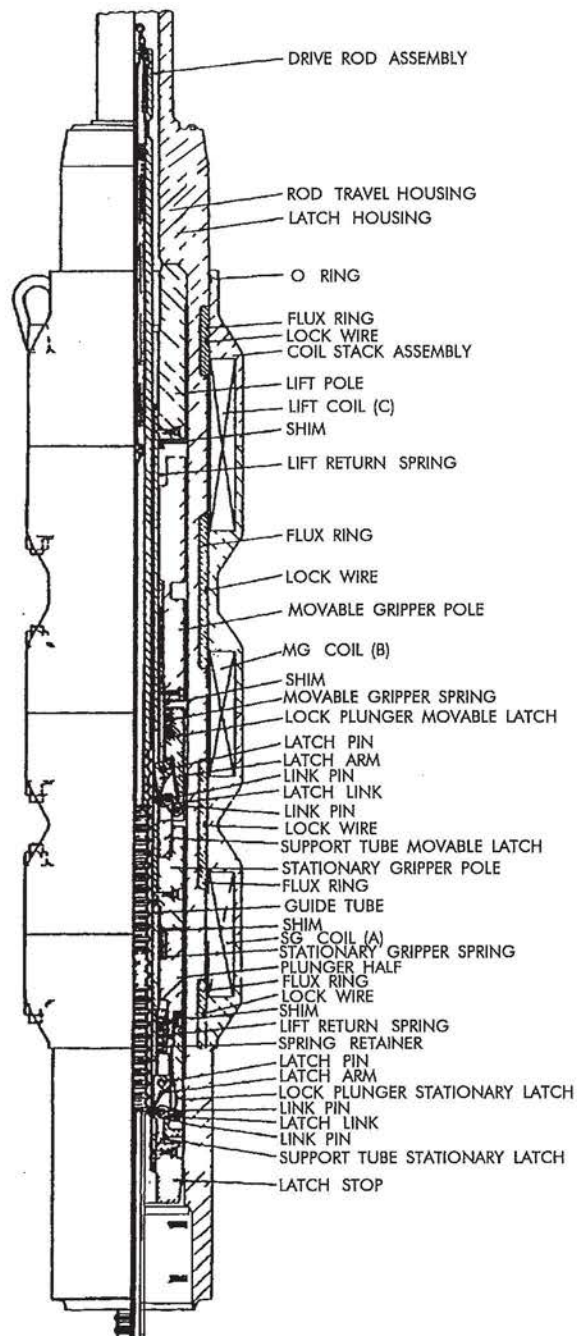


CYCLIC FATIGUE DESIGN CURVE FOR IRRADIATED ZIRCALOY  
 -2 OR - 4 ROOM TEMPERATURE TO 600° F (316° C). TOTAL  
 IRRADIATION EXPOSURE  $5.5 \times 10^{21}$  nvt FAST FLUENCE ( $>0.625$  eV )



01047869

FIGURE 3.5-1



CONTROL ROD DRIVE MECHANISM SCHEMATIC

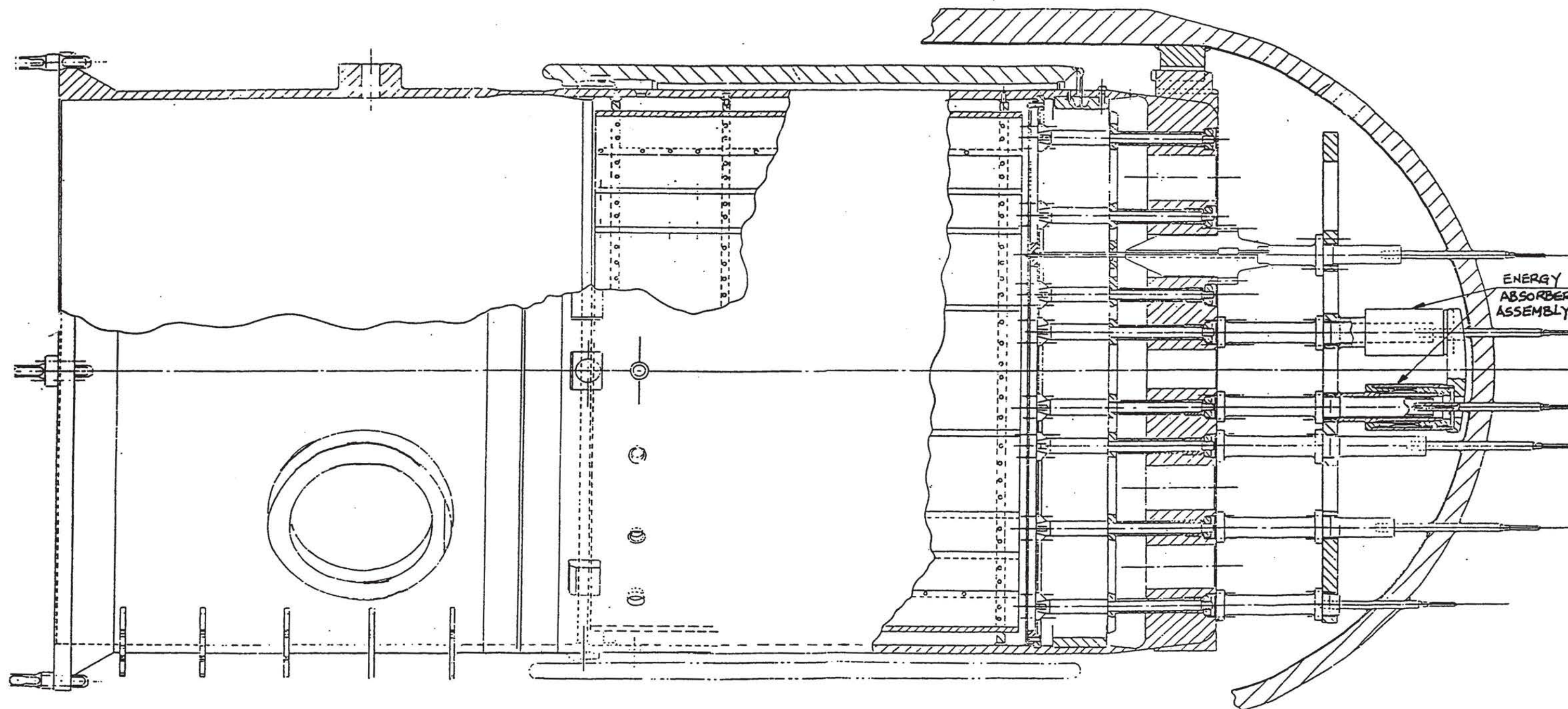
DRAWN BY: VLS	DATE: 1-16-07	NORTHERN STATES POWER COMPANY <i>XcelEnergy</i>	SCALE: NA	REVISION: 29
PAGE. NO. NA	CAD-FILE U03502.DGN	PRAIRIE ISLAND NUCLEAR GENERATING PLANT RED WING, MINNESOTA	<b>FIGURE 3.5-2 REV. 29</b>	

CAD FILE: J / CAD / PRI / ISFSI\_SAR / U03502.DGN

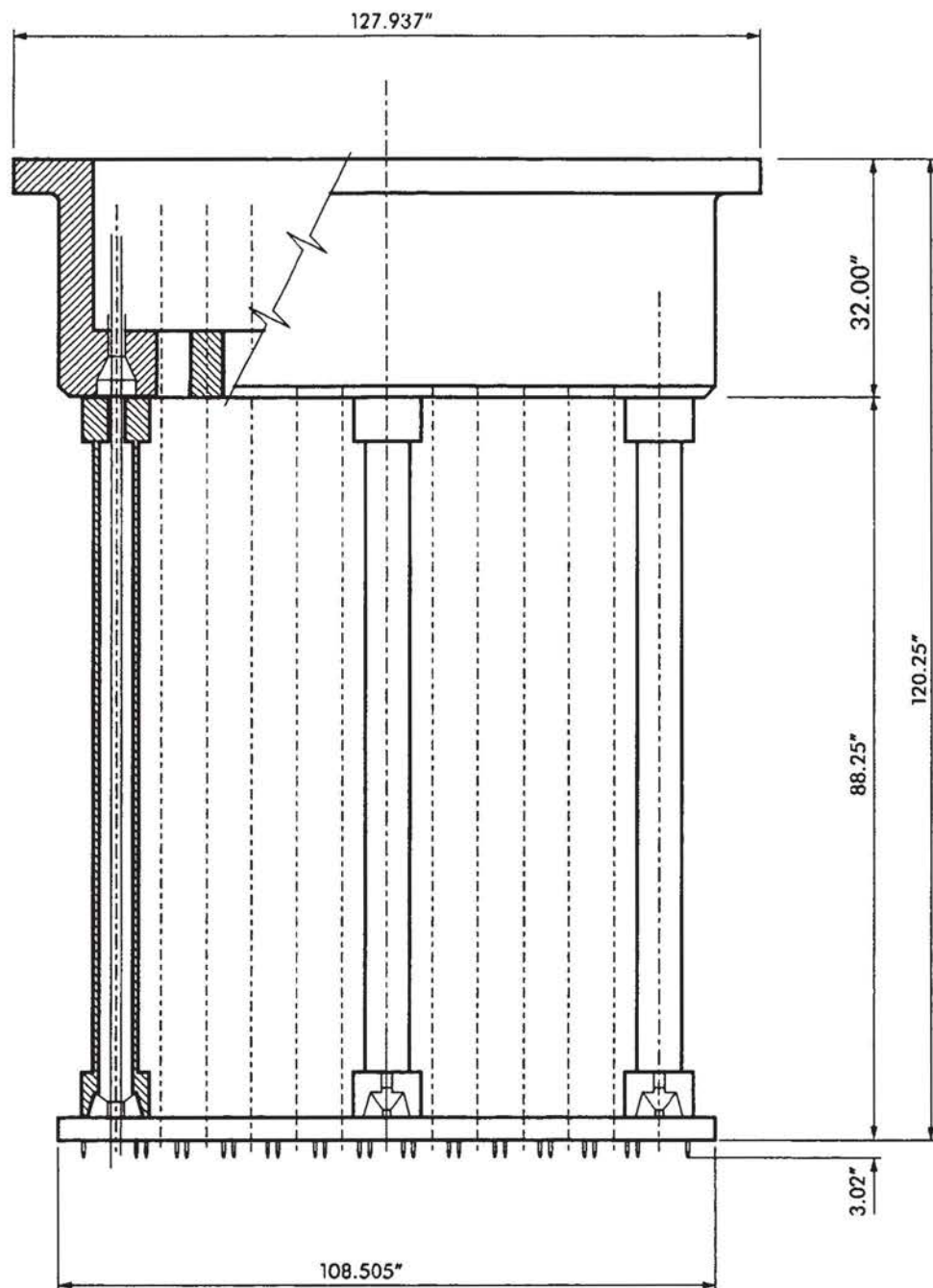
01047869

FIGURE 3.5-2





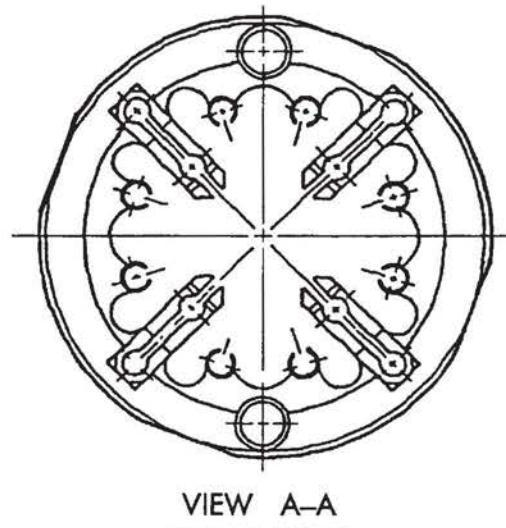
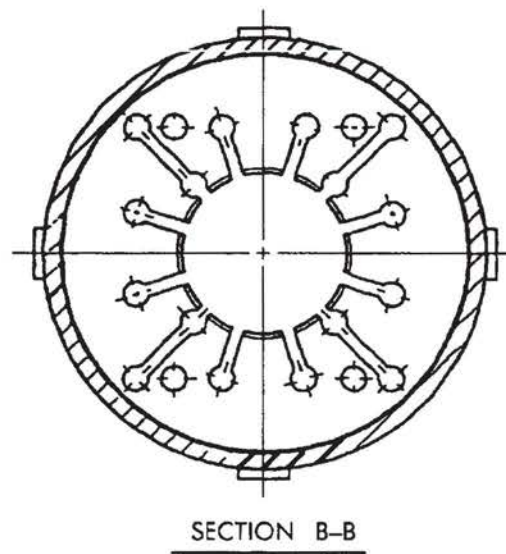
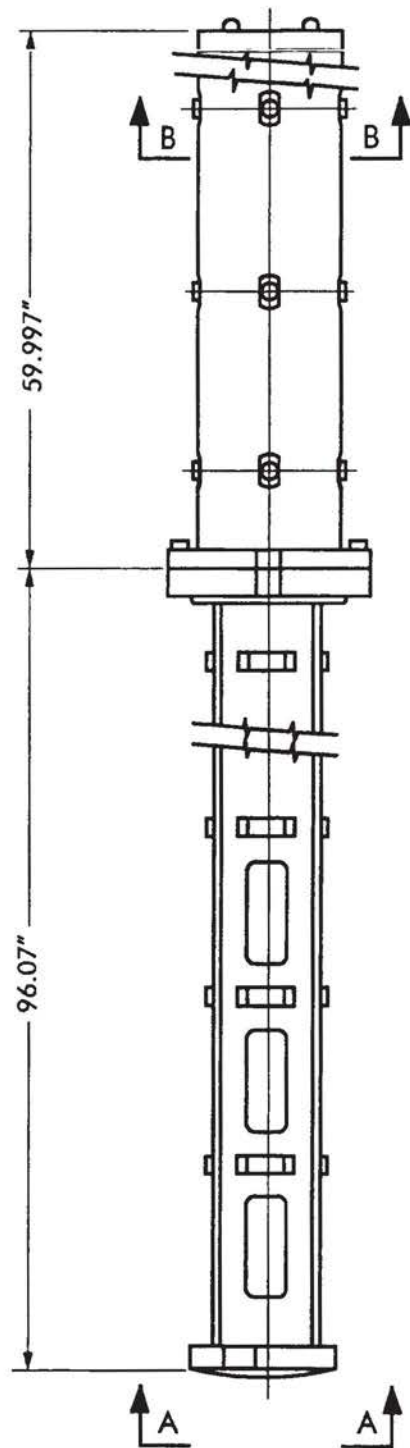
DWN TAM	DATE 6-23-99	SIGNIFICANT NO.									
CHECKED		GROUP									
PROJECT NO. ETNSUR		1	2	3	4	5	CL	6			
APP'D & CERT.		LOWER CORE SUPPORT STRUCTURE									
CAD FILE: U03601.DGN											
NORTHERN STATES POWER COMPANY		SCALE NONE		REV							
PRAIRIE ISLAND NUCLEAR GENERATING PLANT				FIGURE 3.6-1 REV. 18							
RED WING, MINNESOTA											



# REACTOR VESSEL UPPER INTERNALS

DWN T. MILLER	DATE 6-23-99	NORTHERN STATES POWER COMPANY PRAIRIE ISLAND NUCLEAR GENERATING PLANT RED WING MINNESOTA	SCALE: NONE	
CHECKED	CAD FILE U03602.DGN		<b>FIGURE 3.6-2 REV. 18</b>	





# GUIDE TUBE ASSEMBLY

DWN T. MILLER	DATE 6-23-99	NORTHERN STATES POWER COMPANY PRAIRIE ISLAND NUCLEAR GENERATING PLANT RED WING MINNESOTA	SCALE: NONE	FIGURE 3.6-3 REV. 18
CHECKED	CAD FILE U03603.DGN			



**FIGURE 3.6-4, DELETED**